Manufacturing & Service Operations Management

Publication details, including instructions for authors and subscription information:
http://pubsonline.informs.org

On the Values of Vehicle-to-Grid Electricity Selling in Electric Vehicle Sharing

Yiling Zhang, Mengshi Lu, Siqian Shen

To cite this article:
Yiling Zhang, Mengshi Lu, Siqian Shen (2020) On the Values of Vehicle-to-Grid Electricity Selling in Electric Vehicle Sharing. Manufacturing & Service Operations Management

Published online in Articles in Advance 30 Mar 2020

. https://doi.org/10.1287/msom.2019.0855

http://pubsonline.informs.org/journal/msom

MANUFACTURING & SERVICE OPERATIONS MANAGEMENT
Articles in Advance, pp. 1–20
ISSN 1523-4614 (print), ISSN 1526-5498 (online)

On the Values of Vehicle-to-Grid Electricity Selling in Electric Vehicle Sharing

Yiling Zhang,[a] Mengshi Lu,[b] Siqian Shen[c]

[a] Department of Industrial and Systems Engineering, University of Minnesota, Minneapolis, Minnesota 55455; [b] Krannert School of Management, Purdue University, West Lafayette, Indiana 47907; [c] Department of Industrial and Operations Engineering, University of Michigan, Ann Arbor, Michigan 48109

Contact: yiling@umn.edu, https://orcid.org/0000-0002-1077-198X (YZ); mengshilu@purdue.edu, https://orcid.org/0000-0002-5961-722X (ML); siqian@umich.edu, https://orcid.org/0000-0002-2854-163X (SS)

Received: May 8, 2018
Revised: April 13, 2019; September 3, 2019; September 11, 2019
Accepted: September 13, 2019
Published Online in Articles in Advance: March 30, 2020

https://doi.org/10.1287/msom.2019.0855

Abstract. ***Problem definition***: We study electric vehicle (EV) sharing systems and explore the opportunity for incorporating vehicle-to-grid (V2G) electricity selling in EV sharing. ***Academic/practical relevance***: The problem involves complex planning and operational decisions, as well as multiple sources of uncertainties. The related optimization models impose significant computational challenges. The potential value of V2G integration may have far-reaching impacts on EV sharing and sustainability. ***Methodology***: We formulate the problem as a two-stage stochastic integer linear program. In the first stage, we optimize decisions related to service planning, the capacity of parking and charging facilities, EV battery capacities, and EV allocation in each zone under uncertain time-dependent trip demand and electricity prices. In the second stage, for a realized demand–price scenario, we construct a time-and-charging-status expanded transportation network and optimize operations of the shared vehicle fleet, EV battery charging, and V2G selling. We develop Benders decomposition and scenario decomposition approaches to improve computational efficiency. A linear-decision-rule-based approximation approach is also provided to model dynamic operations. ***Results***: Via testing instances based on real-world and synthetic data, we demonstrate the computational efficacy of our approaches and study the benefits of integrating V2G in EV sharing from the service provider, consumer, and socioenvironmental aspects. ***Managerial implications***: V2G integration can significantly increase the profitability of EV sharing and the quality of service. It results in the preference of larger EV fleets and battery capacities, which further leads to various socioenvironmental benefits. The benefit of V2G can still prevail, even with more severe battery degradation and can be more significant when combined with (i) more stringent service levels, (ii) more traffic congestion, or (iii) urban spatial structures with concentrated business/residential areas. V2G integration (complemented by fast charging technology) can also benefit carshare users through improvement in the quality of service.

Funding: This work was supported by the National Science Foundation [Grants CMMI-1727618, CMMI-1727478, and ECCS-1709094].
Supplemental Material: The online appendices are available at https://doi.org/10.1287/msom.2019.0855.

Keywords: sustainable transportation • energy systems • electric vehicle sharing • vehicle-to-grid • stochastic integer programming • decomposition algorithms

1. Introduction

The concept of a sharing economy introduces new business models serving as middle grounds between public transportation and private vehicle ownership. Growing environmental consciousness and the rising cost of vehicle ownership have also accelerated the introduction and adoption of carsharing as a means of reducing greenhouse gas (GHG) emissions, traffic congestion, as well as transportation expenses. Indeed, the carsharing industry has been booming recently, as it provides a flexible transport means and affordable vehicle access for individual customers.

Driven by government subsidies, tightened regulations on fuel economy, and advances in sustainable energy technologies, the development of electric vehicles (EVs) is transforming the automotive industry, including the evolution of carsharing. EV sharing programs are currently implemented in several major cities around the globe (e.g., BlueLA in Los Angeles, WE in Berlin, and EVCard in Shanghai) and provide effective ways to achieve cleaner transportation. Meanwhile, vehicle-to-grid (V2G) technology allows EVs to communicate with the power grid to release stored energy back to the grid, making renewable

sources even more diffused and affordable. V2G integration has received widespread and enthusiastic support from the automobile and energy industries as well as from government agencies. For example, Southern California Edison, a primary regional electricity supplier, partnered with the Department of Defense to test a V2G pilot project at the Los Angeles Air Force Base and reported positive results (Douris 2017). The Japanese automobile manufacturer Nissan has secured regulatory approval in Germany for its LEAF EVs to provide electricity to the grid, hoping to attract corporate fleet customers with more than 60 EVs (Steitz 2018).

1.1. Motivation and Research Questions

In this paper, we aim to investigate, from an operations management point of view, the potential effects and benefits of incorporating V2G electricity selling in EV sharing, categorized as follows.

1.1.1. Carshare Service Providers and User Benefits. For carsharing service providers, the primary benefit from V2G integration is the additional revenue generated by selling stored electricity in EVs back to the grid. However, many important questions remain unanswered. How much revenue can be generated? How will V2G integration interact with regular carsharing operations? We will quantify the revenue increase due to V2G and study its impact on the carshare business.

1.1.2. Carshare User Benefits. For carshare users, one concern about V2G is that it may reduce vehicle accessibility and, therefore, lower the quality of service. However, the introduction of V2G will affect the service provider's planning and operational decisions, which may in turn increase or decrease vehicle accessibility. We will investigate whether V2G will actually benefit the carshare users with a higher quality of service, after taking all effects into consideration.

1.1.3. Socioenvironmental Benefits. Carsharing is effective in reducing private vehicle ownership and, when equipped with EVs, it can further reduce GHG emissions and pollution. Studies have shown that each vehicle added to a carshare fleet can reduce up to 15 private cars (Bondorová and Archer 2017), and replacing each conventional car with an EV results in a decrease of CO_2 emissions by 31 tons over the entire life cycle of a vehicle (Aguirre et al. 2012). The key to these benefits is deploying more EVs to a carshare fleet. We will study how V2G integration affects the fleet size, which then translates into socioenvironmental impacts.

1.1.4. Electrical Grid Benefits. On a daily basis, one EV can provide enough electricity to meet as much as one household's demand. EVs can also be used as storage device against energy shortage. In 2015, the automaker Nissan announced a major V2G trial project in France, claiming that, in a future in which all vehicles are EVs, the V2G system can be a virtual power plant that can exceed the current electricity generation capacity in that country by threefold.[1] With more shared EV fleets and their available storage, power grid operators can have more flexibility in generating power and lowering electricity price, even during peak load hours. However, it is unknown whether similar benefits can be achieved with a typical carshare fleet, especially when V2G may interfere with regular rental operations. We will evaluate the potential of V2G integration in carshare systems.

1.2. Methodology Overview

For system planning under uncertainty, a common method is to consider a two-stage stochastic optimization problem in which long-term (planning) decisions are made before knowing the realizations of uncertain parameters, and short-term (operational) decisions respond to individual realizations and are solved to obtain a value function of first-stage decisions.

We formulate a two-stage stochastic integer linear programming model to optimize planning decisions for opening service zones, parking and charging facility capacity design, EV fleet allocation, and EV battery capacity selection. In practice, the planning decisions are often made monthly, quarterly, or even yearly and cannot be easily changed on a daily basis. We assume that all the planning decisions are made on a yearly basis. The carsharing demand and electricity price vary throughout a day, and we optimize vehicle rental, relocation, charging, and electricity selling based on first-stage planning decisions and each possible realization generated independently from an underlying joint distribution of the two uncertainties. (In this paper, we assume that the full distributional information is known, which can be obtained from historical data, and we employ the sample average approximation approach; see Kleywegt et al. 2002.) We scale both of the first-stage and second-stage cost parameters to daily cost and minimize a weighted sum of the total planning cost of building an integrated EV sharing system and the expected operational cost for operating and charging EVs and selling electricity. In particular, our first-stage variables are purely integral, and, for each realization, we construct a spatial-temporal state-of-charge (SoC) network to optimize operational decisions using linear programming in the second stage.

Two solution approaches are proposed for speeding up the process of solving the overall stochastic integer program model with many parallel subproblems. We first employ the Benders decomposition

algorithm (Benders 1962, Birge and Louveaux 2011) to seek valid inequalities for lower-bounding the second-stage value function based on dual extreme-point solutions. Alternatively, we link the first-stage integer decision variables in each subproblem via nonanticipativity constraints and propose using scenario decomposition (Ahmed 2013) to derive upper and lower bounds of the optimal objective value using optimal scenario-based first-stage solutions. Moreover, a linear-decision-rule-based approximation approach is presented in Online Appendix E, where we interpret the second-stage decisions as linear functions of segregated uncertainties and solve the overall problem as an integer linear program. This approach allows us to easily implement the recourse decisions in individual scenarios according to observed realizations of the uncertainties.

1.3. Contributions and Main Results

The main contributions of the paper are threefold.

1. We present a new model for EV sharing systems integrated with V2G procedures. We formulate a two-stage stochastic integer programming model to optimize carshare fleet planning, including service coverage, EV (battery/range) choice, and fleet deployment, under two uncertainties from carsharing demand and seasonal electricity price.

2. Via numerical studies based on real-world data, we investigate the benefits of integrating V2G selling in EV sharing, as outlined in Section 1.1. Aside from increasing the service provider's revenue, integrating V2G in EV sharing has other benefits, such as complementing the use of fast charging and inducing more vehicle deployment and the preference of larger batteries, as illustrated in Figure 1. Furthermore, we find that the benefits of V2G can endure higher battery degradation cost and can be even more significant when combined with fast charging technology, more stringent service-level requirements, more severe traffic congestion, or concentrated residential/business areas in urban spatial structures.

3. We demonstrate the computational efficacy of using decomposition approaches, including Benders decomposition and scenario decomposition, for optimizing the two-stage stochastic integer programming model with large-scale spatial-temporal-SoC networks in the second stage and a large number of operational decision variables in each network. We further provide an adaptive approach based on a linear-decision-rule approximation, for implementing the operational decisions according to future realizations of uncertainty. The solution methods are general and can be applied to other stochastic resource planning and system design problems.

Figure 1. Illustration of the Benefits of Integrating V2G in EV Sharing

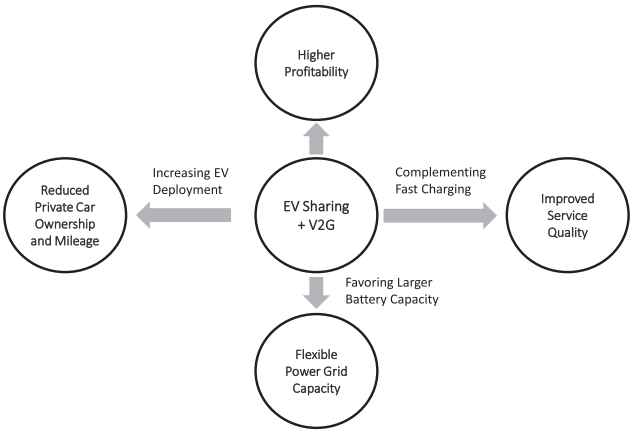

1.4. Structure of the Paper

The remainder of the paper is organized as follows. In Section 2, we review related literature on carsharing, EV sharing, and V2G. In Section 3, we describe our problem and formulate the two-stage stochastic programming model with details about spatial-temporal-SoC networks and the related subproblems. In Section 4, we present the details of the Benders and scenario decomposition approaches. We also present a linear-decision-rule-based approximation for easy implementation of recourse decisions, with details given in Online Appendix E. In Section 5, we test diverse instances to demonstrate (i) the computational efficiency of our approaches and (ii) the benefits of integrating EV sharing with V2G. We conclude the paper and discuss future research directions in Section 6. For the simplicity of tracking notation, we summarize all of the notation in Table A.1 in Online Appendix A.

2. Literature Review

We review the related literature in the design and operations of general carsharing and EV sharing systems using mathematical optimization approaches and the related studies on the economics and operations of V2G, especially on V2G integration in EV sharing systems.

2.1. Carsharing

Carsharing programs were introduced in Europe in the 1950s, but not until the late 1980s were they widely adopted due to the advancement of communication technology (Shaheen et al. 1998). Barth and Todd (1999) were among the first to use quantitative methods for evaluating benefits and drawbacks of carsharing systems. They developed a simulation model to evaluate operational issues, including vehicle availability, vehicle distribution, and energy management, under different demand travel patterns.

Barrios and Godier (2014) developed an agent-based simulation model of a flexible carsharing system to explore trade-offs between fleet size and vehicle relocation. To obtain minimum-cost vehicle relocation plans for vehicle sharing systems, Nair and Miller-Hooks (2011) solved a stochastic mixed-integer linear programming (MILP) model with joint chance constraints to ensure high-demand satisfaction rates under uncertain carsharing demand. Benjaafar et al. (2017b) studied inventory positioning in a product rental network, which also applies to carsharing. He et al. (2020) studied a vehicle repositioning problem to minimize the total cost of repositioning and lost sales by solving a multistage distributionally robust optimization model with an enhanced linear decision rule.

Recently, Lu et al. (2018) considered a fleet management problem under uncertain trip demand. They employed a two-stage stochastic MILP model, in which they decide strategic decisions, including those pertaining to station locations and fleet sizes, before realizing the uncertain demand. In this paper, we further extend their work to EV sharing systems by explicitly modeling the EV charging and V2G selling processes, as well as the battery capacity choices of the EV fleet. The new features of charging and V2G increase the problem complexity and motivate us to develop more efficient algorithms. Also, the introduction of V2G technology restricts the vehicle availability to customers and thus makes the profitability and socioenvironmental impact of EV sharing unclear, which inspires our work.

Another branch of literature about *servicization*, a business model concept, under which a firm sells the use of a product rather than the product itself, is also related to carsharing. Agrawal and Bellos (2016) studied the conditions where the servicization can be environmentally beneficial. Bellos et al. (2017) considered profitability and the environmental impact of carsharing provided by an automobile manufacturer that designs its product line to trade off between fuel efficiency and driving performance. There is a growing body of literature focusing on peer-to-peer carsharing, where the users can make decisions either as an owner or a renter. We refer readers to Benjaafar et al. (2017a, 2019) for more discussion on modeling, ownership, usage, and social welfare.

2.2. EV Sharing

Barth and Todd (1999) studied operational issues related to EV availability, EV distribution, and energy management when integrating EVs into carsharing systems. In EV sharing, when making strategic planning decisions, operators also need to consider charging requirements for shared EVs, including charging stations, charging duration and amount, and so on. Mak et al. (2013) studied infrastructure planning for EVs with battery swapping. Boyacı et al. (2015) proposed a multiobjective MILP model for station-based one-way carsharing. They identify potential station locations by solving a set cover problem and optimize the net benefits of both the operator and users. However, in their model, only the charging duration is modeled, but energy consumption levels of individual EVs are neglected. Biondi et al. (2016) developed a two-step optimization approach to minimize charging costs when the power-sharing technology is employed, to allow multiple EVs to be charged simultaneously in one charging station. He et al. (2017) develop a model to trade off between maximizing customer adoption and minimizing operation costs under imbalanced travel patterns. They formulate a second-order conic program to model customer adoption rates and model fleet operations in a queuing network with four states: idle, rental, repositioning, and recharging. He et al. (2018) further considered more detailed charging operations using queueing analysis. To the best of our knowledge, none of the above works considers the V2G selling option for shared EV systems, which can significantly impact EV fleet size as well as the service level of EV sharing systems.

2.3. V2G

Enabled by new technologies, EVs can serve as distributed energy resources to feed electricity back to the grid when needed. This service provided by EVs is known as V2G, of which the concept has been studied from different aspects, including social barriers, social welfare benefits, potential for supplying electricity markets, and other issues (see, e.g., Sovacool and Hirsh 2009, Kempton and Tomić 2005, Lund and Kempton 2008, Turton and Moura 2008, Peterson et al. 2010, Tan et al. 2016). To make the V2G concept practical, the first step is to consolidate a large number of EVs, due to individual EVs' small battery capacities. Carsharing fleets provide a means to aggregate EVs as virtual power plants, and thus they are utilized to generate revenue through the administration of frequency and voltage. On the other hand, carsharing may increase the operation time of EVs, which is against the motivation behind V2G to take advantage of the under-utilization of EVs. Such business models have been discussed in recent publications (e.g., Fournier et al. 2015, 2014; Lauinger et al. 2017), but the profitability of V2G in carsharing systems is not clear and the model has not been quantitatively verified, due to the complexity of mathematical models, especially under stochastic demand and electricity price. This motivates our study in this paper.

3. Problem Description and Formulation

We consider service zone planning and fleet management in EV sharing. We particularly focus on the impact of integrating V2G by taking into account uncertainties of carsharing demand and electricity price. Specifically, we consider a reservation-based EV system for finite time periods. The service region is discretized into small zones with different costs of operating and acquiring parking facilities. The parking, charging, and V2G facilities have capacity limits, and both the costs and capacities may be different from zone to zone. In each time period, we assume that any excess demand in a zone is lost immediately if the demand exceeds the number of available EVs.

To solve the problem, we formulate a two-stage stochastic integer programming model, where strategic decisions are determined in the first stage, including choices of which zones to serve, EV battery capacity choices, the number of EVs deployed in each service zone, and the capacities of parking spaces with or without the function of charging and/or V2G. In the second stage, a recourse problem is solved to approximate the expected cost of operating the designed system over all time periods, given the strategic and tactical decisions made in the first stage.

Remark 1. Although the nature of the problem—having rental requests over time—leads to a multistage dynamic model, in this paper, we consider a two-stage stochastic programming model to focus on resource planning and its cost estimation, by aggregating all recourse decisions and system uncertainties in the second-stage problem. Such a two-stage approximation has been widely employed to model multistage dynamics. For example, Cheung and Chen (1998) considered a container allocation problem, assuming that all random parameters are realized in the second stage. In another example, Salmerón and Apte (2010) solved natural disaster asset prepositioning using a two-stage stochastic program with the first-stage decisions as the resource expansion and the second-stage decisions as resource allocation and transportation after disasters.

3.1. First-Stage Problem and Formulation

Consider a set $\mathcal{I}$ of potential service zones and binary planning decision variables z_i, $\forall i \in \mathcal{I}$, such that $z_i = 1$ indicates that zone i is served and $z_i = 0$ otherwise. We consider three types of parking capacities: (i) type P: solely parking space; (ii) type C: parking space with charging stations; and (iii) type S: parking space with charging stations having bidirectional power flow interfaces that allow electricity to flow into and out of EVs. Let $\mathcal{K} = \{\text{P, C, S}\}$ be the set of all parking space types. The integer variable s_i^k indicates the number of type k parking spaces operated in zone $i \in \mathcal{I}$. There are several business models regarding ownership and accessibility of EV charging stations. For example, car2go in San Diego used to pay a third-party charging network (i.e., ECOtality) for using its charging infrastructure. On the other hand, Autolib in Paris installed and operated its own network of charging stations that is also available to the public. In this paper, we assume that the service providers install their own charging stations. Moreover, we consider a set $\mathcal{E}$ of vehicle battery capacity choices. We also assume that battery capacities are the same across the entire fleet, since having homogeneous vehicle fleets is common in existing carsharing systems. For example, car2go operates purely electric fleets with the same Smart Fortwo electric vehicles in Amsterdam and Madrid.[2] Let σ_e denote the battery capacity decision such that $\sigma_e = 1$ if chosen and $\sigma_e = 0$ otherwise for all $e \in \mathcal{E}$. Throughout this paper, as a convention, we use boldface letters to denote vectors of corresponding variables; that is, $\mathbf{z} = (z_i, i \in \mathcal{I})^\mathsf{T}$, $\mathbf{s} = (s_i^k, k \in \mathcal{K}, i \in \mathcal{I})^\mathsf{T}$, and $\sigma = (\sigma_e, e \in \mathcal{E})^\mathsf{T}$.

The service coverage, the number of parking/charging facilities, and the battery capacity choice decisions are strategic decisions that must be consistent over long terms. Vehicle deployment, on the other hand, can be adjusted in shorter periods (e.g., in each season) to cope with varying business conditions. We further consider the case where rental demand and/or electricity prices may have significant seasonality. Let $\mathcal{H} = \{1, \ldots, H\}$ denote the set of "seasons." Let $x_{e,i}^h$ denote the number of vehicles with battery capacity e allocated to service zone i during season h, and let $\mathbf{x}_e^h = (x_{e,i}^h, i \in \mathcal{I})^\mathsf{T}$.

We associate the planning variables z_i, $x_{e,i}^h$, and s_i^k with unit costs c_i^F, $c_{e,i}^\mathrm{V}$, and c_i^k, respectively. Here, c_i^F is the fixed cost of opening service zone i, $c_{e,i}^\mathrm{V}$ represents the cost of allocating one EV in zone i, and c_i^k is the cost of acquiring one type k parking space in zone i, for all $i \in \mathcal{I}$.

Given the first-stage decision inputs, let $Q_e^h(\mathbf{x}_e^h, \mathbf{z}, \mathbf{s})$ be the expected value of the total operational cost plus demand loss penalty, minus revenue in season h, with battery capacity e. We denote $o_h \geq 0$ as the weight associated with the cost incurred in season h such that $\sum_{h\in\mathcal{H}} o_h = 1$. We formulate the overall model as follows:

$$\min_{\mathbf{z},\mathbf{s},\sigma,\mathbf{x}} \sum_{i\in\mathcal{I}} \left(c_i^\mathrm{F} z_i + \sum_{k\in\mathcal{K}} c_i^k s_i^k + \sum_{h\in\mathcal{H}, e\in\mathcal{E}} c_{e,i}^\mathrm{V} x_{e,i}^h \right) + \sum_{h\in\mathcal{H}, e\in\mathcal{E}} \sigma_e o_h Q_e^h\left(\mathbf{x}_e^h, \mathbf{z}, \mathbf{s}\right) \tag{1a}$$

$$\text{s.t. } s_i^k \leq M_i^k z_i, \qquad \forall i \in \mathcal{I}, \forall k \in \mathcal{K}, \tag{1b}$$

$$\sum_{e\in\mathcal{E}} \sigma_e = 1, \tag{1c}$$

$$x^h_{e,i} \le \sum_{k\in\mathcal{K}} M^k_i \sigma_e, \quad \forall e \in \mathcal{E},\ \forall h \in \mathcal{H},\ \forall i \in \mathcal{I}, \tag{1d}$$

$$x^h_{e,i} \le \sum_{k\in\mathcal{K}} s^k_i, \quad \forall e \in \mathcal{E},\ \forall h \in \mathcal{H},\ \forall i \in \mathcal{I}, \tag{1e}$$

$$z_i, \sigma_e \in \{0,1\}, s^k_i, x^h_{e,i} \in \mathbb{Z}_+ \cup \{0\}, \quad \forall e \in \mathcal{E}, \forall h \in \mathcal{H}, \forall i \in \mathcal{I},\ \forall k \in \mathcal{K}. \tag{1f}$$

The objective function (1a) minimizes the sum of the total cost of planning service zones, acquiring EVs and parking spaces with charging and V2G-selling abilities, and the expected operational cost $Q^h_e(\mathbf{x}^h_e, \mathbf{z}, \mathbf{s})$ over all time periods, of which we will present a detailed formulation in Section 3.3. Constraints (1b) require that parking spaces and EVs can only be deployed in served zones, where the big-M coefficient M^k_i is set as the maximum capacity of type k parking space in zone i, for all $i \in \mathcal{I}$, $k \in \mathcal{K}$, which is subject to investment budget and/or government policy. Constraints (1c)–(1d) ensure that only one battery capacity is selected for all EVs. Constraints (1e) require that the number of EVs deployed in each zone must be no more than the total number of parking spaces (of all types) allocated in that zone, for all zones. Constraints (1f) enforce binary values of z-variables and nonnegative integer values of s- and x-variables.

3.2. Spatial-Temporal-SoC Network

Given the first-stage decisions $(\mathbf{x}^h_e, \mathbf{z}, \mathbf{s})$, we optimize EV operations, including rental, charging, relocation, and V2G selling, over each spatial-temporal-SoC network $\mathcal{G} = (\mathcal{N}, \mathcal{A})$ in the second-stage problem, modeled as $Q^h_e(\mathbf{x}^h_e, \mathbf{z}, \mathbf{s})$. Let $\mathcal{T} = \{1, \dots, T\}$ be the set of time periods for which we operate the designed EV sharing system, and let $\mathcal{B}_e = \{0, 1, \dots, e\}$ be the set of SoC levels. Let $\mathcal{I}_z = \{i \in \mathcal{I} : z_i = 1\}$ denote the set of zones to serve according to decision $\mathbf{z}$.

Let $\widetilde{d}_{ijts}$ be the number of trips requested from zone i to zone j at time t that need to be completed by time s, where $s \ge t + l_{ij}$, where $l_{ij} > 0$ is the shortest traveling time from zone i to j. For all zones, we denote unit electricity prices of charging and V2G selling by $\widetilde{p}^{C,h}_t$ and $\widetilde{p}^{S,h}_t$ for each time period $t \in \mathcal{T}$ (in season $h \in \mathcal{H}$), respectively. Let $\widetilde{\mathbf{d}} = (\widetilde{d}_{ijts}, \forall i, j \in \mathcal{I}_z, t, s \in \mathcal{T})^\mathsf{T}$ be the vector of spatial-temporal demand. We denote $\widetilde{\mathbf{p}}^{C,h} = (\widetilde{p}^{C,h}_t,\ t \in \mathcal{T})^\mathsf{T}$ and $\widetilde{\mathbf{p}}^{S,h} = (\widetilde{p}^{S,h}_t,\ t \in \mathcal{T})^\mathsf{T}$ as the vectors of electricity buying and selling prices, respectively. Given the first-stage decisions $(\mathbf{x}^h_e, \mathbf{z}, \mathbf{s})$, the network $\mathcal{G}$ is constructed for each realization of uncertain parameters $(\widetilde{\mathbf{d}}, \widetilde{\mathbf{p}}^{C,h}, \widetilde{\mathbf{p}}^{S,h})$.

Throughout this paper, we assume that, for each EV, the SoC changes linearly in time for both charging and discharging processes, and we present the details of SoC modeling in Online Appendix B. We assume that an EV cannot be rented or relocated when the SoC falls below a given threshold level and must be idle or charged in the current zone. The SoC consumption of driving is assumed to be linear with the traveling time (or, equivalently, the traveling distance following the justification in Zhou et al. 2011), and we denote the number of SoC units consumed per time period b^D. Let b^C (b^S) be the number of SoC units increased (decreased) by one time period of charging (discharging). Because a battery's service life degrades due to repeating charge/discharge cycles (Kempton and Tomić 2005, Peterson et al. 2010, Zhou et al. 2011), following Peterson et al. (2010), we assume that the degradation cost is proportional to the number of SoC units increased (decreased). Each unit of SoC change incurs a unit degradation cost c^{deg}_e, where e is the chosen battery capacity. Let r_{ij} be the revenue per period generated by one trip from zone $i \in \mathcal{I}$ to zone $j \in \mathcal{I}$. The operational costs include the cost of relocating EVs from zone i to zone j, denoted by $c^{relo}_{ij} \ge 0$ per vehicle per period, and the cost incurred when EVs are idle in zone i, denoted by $c^{idle}_i \ge 0$ per vehicle per period.

We use the term "movements" to denote changes of EV states, and we use arcs $a \in \mathcal{A}$ to represent all movements in $\mathcal{G}$. We let node $n_{itb} \in \mathcal{N}$ represent a state of EVs, that is, being in location $i \in \mathcal{I}_z$ at time $t \in \mathcal{T}$ with SoC $b \in \mathcal{B}_e$, and we construct arcs in-between pairs of nodes with all possible transitions between their corresponding states. We consider the following five types of arcs in $\mathcal{A}$:

1. **Rental arcs** $a = (n_{itb}, n_{jsb'}) \in A^{rent}$ for $\widetilde{d}_{ijts} > 0$, $b' \ge 0$, and $s - t \ge l_{ij}$, with capacity $\widetilde{d}_{ijts}$ and cost $-r_{ij}(s-t)$ per unit flow. To be a rental arc, the relation between b and b' needs to satisfy $b - b' \ge (s-t)b^D$, and b should also be above the minimum required driving SoC level threshold. Flows on these arcs represent EVs with SoC $b > 0$ being rented from zone i starting from period t, and returned to zone j in period s with the SoC level being b'. Let $\mathcal{D}^{rent}_{ijts} = \{(n_{itb}, n_{jsb'}) \in \mathcal{A}^{rent} :\ b' \ge 0\}$, and note that the combined capacity of all arcs in $\mathcal{D}^{rent}_{ijts}$ is $\widetilde{d}_{ijts}$.

2. **Relocation arcs** $(n_{itb}, n_{j,t+l_{ij},b'}) \in A^{relo}$ for $b' \ge 0$ and $1 \le t \le T - l_{ij}$, with infinite capacity and cost $c^{relo}_{ij} l_{ij}$ per unit flow. The SoC levels need to satisfy $b \ge b' + l_{ij}b^D$, and the SoC level b has to be above the driving threshold SoC level. Flows on the arcs represent EVs with SoC $b > 0$ being relocated from zone i in period t, and arriving at zone j in period $t + l_{ij}$ with the ending SoC equal to b'.

3. **Idle arcs** $(n_{itb}, n_{i,t+1,b}) \in A^{idle}$ for zone $i \in I_z$ and period $1 \le t \le T$, with cost c^{idle}_i per unit flow. Flows on these arcs represent EVs being idle (i.e., not involved with either charging or V2G selling) in zone i from period t to $t+1$ with the SoC equal to b. Let $\mathcal{D}^P_{it} = \{(n_{itb}, n_{i,t+1,b}) \in \mathcal{A}^{idle} :\ b \in \mathcal{B}_e\}$. We note that the combined capacity of all arcs in $\mathcal{D}^P_{it}$ is $\sum_{k\in\mathcal{K}} s^k_i$, since

an idle EV is allowed to park in a parking space of any type.

4. **Charging arcs** $(n_{itb}, n_{i,t+1,b+b^C}) \in \mathcal{A}^{\text{charge}}$ for zone $i \in \mathcal{I}_z$, $0 \le b + b^C < e$, and period $0 \le t \le T-1$, with cost $\widetilde{p}_t^{C,h} + c_e^{\text{deg}}$ per unit flow. Flows on these arcs represent the EVs being charged from b to $b + b^C$ in zone i from period t to $t+1$. Let $\mathcal{D}_{it}^C = \{(n_{itb}, n_{i,t+1,b+b^C}) \in \mathcal{A}^{\text{charge}} : b + b^C \in \mathcal{B}_e\}$ for $t \le T-1$, and the combined capacity of all arcs in $\mathcal{D}_{it}^C$ is $s_i^C + s_i^S$. Here we may have several options for b^C, representing different charging speeds such as regular and fast charging, as mentioned in Section 5.

5. **Selling arcs** $(n_{itb}, n_{i,t+1,b-b^S}) \in \mathcal{A}^{\text{sell}}$ for zone $i \in \mathcal{I}_z$, $0 \le b - b^S$, and period $t \le T-1$, with cost $-\widetilde{p}_t^{S,h} + c_e^{\text{deg}}$ per unit flow. Flows on these arcs represent EVs selling electricity back to the grid in zone i from period t to $t+1$ and the SoC decreasing from b to $b - b^S$. Let $\mathcal{D}_{it}^S = \{(n_{itb}, n_{i,t+1,b-b^S}) \in \mathcal{A}^{\text{sell}} : b - b^S \in \mathcal{B}_e\}$ for $t \le T-1$ and the combined capacity of $\mathcal{D}_{it}^S$ is s_i^S.

The combined capacity of all arcs in set $\cup_{k\in\mathcal{K}}\mathcal{D}_{it}^k$ is $\sum_{k\in\mathcal{K}} s_i^k$. The set $\mathcal{A}$ is the union of the five types of arcs; that is, $\mathcal{A} = \mathcal{A}^{\text{rent}} \cup \mathcal{A}^{\text{relo}} \cup \mathcal{A}^{\text{idle}} \cup \mathcal{A}^{\text{charge}} \cup \mathcal{A}^{\text{sell}}$. We denote the per-unit net flow cost and the capacity on arc a by c_a^h and u_a, respectively. The notation $u_{\mathcal{D}}$ denotes the combined capacity of arcs in set $\mathcal{D} \subset \mathcal{A}$. The unit flow costs and capacities of all five arc types are summarized in Table 1. Note that, although the relocation arcs have infinite capacity here, the flows over relocation arcs are bounded above due to other arcs' capacities and flow balance constraints (5c). Moreover, because the unit cost of relocation is positive, with the objective of minimizing the total cost, the flow amounts on relocation arcs will be minimized at optimum.

In Figure 2, we illustrate an example of the spatial-temporal-SoC network, with two zones (A and B), four time periods ($\mathcal{T} = \{1,2,3,4\}$), and three SoC levels ($\mathcal{B}_e = \{1,2,3\}$). The numbers alongside different types of arcs indicate a solution of renting, idling, charging, relocating EVs, and selling electricity in different zones and at different time periods. We illustrate all five types of arcs in Figure 2. Note that within the part of the network for the same service zone, we have V2G, idle, and charging arcs, since they are not related to EVs' location transition. Rental and relocation arcs connect two nodes belonging to different zones.

Remark 2. Energy conversion losses may be of interest to study whether charging and V2G are cost-effective (Kempton and Tomić 2005). With the consideration of conversion losses, in order to buy b^C (sell b^S) units of electricity, one needs to buy $b^C/\bar{\mu}$ from (sell $b^S/\bar{\mu}$ to) the grid with $\bar{\mu} \in (0,1)$. It can be integrated in the current model by increasing the unit flow cost of charging arcs to $(\widetilde{p}_t^{C,h} + c_e^{\text{deg}})/\bar{\mu}$ and reducing the unit flow cost to $\bar{\mu}(-\widetilde{p}_t^{S,h} + c_e^{\text{deg}})$.

3.3. Second-Stage Subproblem Formulation

After constructing a spatial-temporal-SoC network $\mathcal{G}$ for each realized demand and electricity price, we calculate recourse decisions $y_a \ge 0$, $\forall a \in \mathcal{A}$, representing EV movements over the network $\mathcal{G}$, including EV rentals, relocation, idling, charging, and returning electricity to the grid. (We relax the integral constraint for y_a, since we use only the subproblem solutions to estimate the expected cost of the first-stage planning decisions in the future. In Section 5.2, we show that the optimal objective value of the linear-programming relaxation is very close to that of the formulation with integer recourse $y_a \in \mathbb{Z}_+$.) We denote by $w_{ijts} \ge 0$, $i,j \in \mathcal{I}_z$, $1 \le t < s \le T$ the slack variables representing total unmet demands on the rental arcs in set $\mathcal{D}_{ijts}^{\text{rent}}$. We denote by $\mathbf{y} = (y_a, a \in \mathcal{A})^T$ and $\mathbf{w} = (w_{ijts}, \text{for } d_{ijts} > 0)^T$ the vectors of recourse decision variables. Let

$$\mathcal{Q}_e^h\left(\mathbf{x}_e^h, \mathbf{z}, \mathbf{s}, \widetilde{\mathbf{d}}, \widetilde{\mathbf{p}}^S\right) = \min_{\mathbf{y},\mathbf{w}}\left\{\mathbf{c}\left(\widetilde{\mathbf{p}}^{S,h}, \widetilde{\mathbf{p}}^{C,h}\right)^T\mathbf{y} + \mathbf{g}^T\mathbf{w} : (\mathbf{y},\mathbf{w}) \in \Upsilon\left(\mathbf{x}_e^h, \mathbf{z}, \mathbf{s}, \widetilde{\mathbf{d}}\right)\right\}, \tag{2}$$

where set $\Upsilon(\mathbf{x}_e^h, \mathbf{z}, \mathbf{s}, \widetilde{\mathbf{d}})$ is the feasible region of $(\mathbf{y},\mathbf{w})$ based on each network $\mathcal{G}$ given the value of random demand $\widetilde{\mathbf{d}}$; we will discuss detailed constraints in $\Upsilon(\mathbf{x}_e^h, \mathbf{z}, \mathbf{s}, \widetilde{\mathbf{d}})$ later. In the objective function, $\mathbf{c}(\widetilde{\mathbf{p}}^{S,h}, \widetilde{\mathbf{p}}^{C,h})$ is the vector of arc costs per unit flow and is a function of $\widetilde{\mathbf{p}}^{S,h}$ and $\widetilde{\mathbf{p}}^{C,h}$, since costs of selling/charging arcs depend on the electricity selling/buying price $\widetilde{\mathbf{p}}^{S,h}$ and $\widetilde{\mathbf{p}}^{C,h}$. The objective cost consists of two parts.

Table 1. Unit Flow Costs and Capacities for Each Arc Type

Types of arc a	Cost per unit flow c_a^h	Combined capacity $u_{\mathcal{D}}$
Rental arc $(n_{itb}, n_{isb'})$	$-r_{ij}(s-t)$	$u_{\mathcal{D}_{ijts}^{\text{rent}}} = \widetilde{d}_{ijts}$
Relocation arc $(n_{itb}, n_{j,t+l_{ij},b'})$	$c_{ij}^{\text{relo}} l_{ij}$	$+\infty$
Idle arc $(n_{itb}, n_{i,t+1,b})$	c_i^{idle}	$u_{\mathcal{D}_{it}^p} = \sum_{k\in\mathcal{K}} s_i^k$
Charging arc $(n_{itb}, n_{i,t+1,b+b^C})$	$\widetilde{p}_t^{C,h} + c_e^{\text{deg}}$	$u_{\mathcal{D}_{it}^C} = s_i^C + s_i^S$
Selling arc $(n_{itb}, n_{i,t+1,b-b^S})$	$-\widetilde{p}_t^{S,h} + c_e^{\text{deg}}$	$u_{\mathcal{D}_{it}^S} = s_i^S$

Figure 2. (Color online) An Example of the Spatial-Temporal-SoC Network

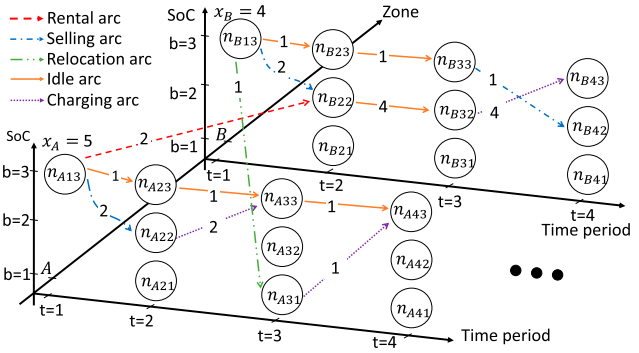

The first term $\mathbf{c}(\widetilde{\mathbf{p}}^{S,h}, \widetilde{\mathbf{p}}^{C,h})^{\mathsf{T}}\mathbf{y}$ is the cost of vehicle movements and the second cost $\mathbf{g}^{\mathsf{T}}\mathbf{w}$ is the penalty from unserved demands with $\mathbf{g}$ being the unit penalty cost vector.

We consider the expected cost

$$Q_e^h(\mathbf{x}_e^h, \mathbf{z}, \mathbf{s}) = \mathbb{E}\left[\mathcal{Q}_e^h\left(\mathbf{x}_e^h, \mathbf{z}, \mathbf{s}, \widetilde{\mathbf{d}}, \widetilde{\mathbf{p}}^{S,h}, \widetilde{\mathbf{p}}^{C,h}\right)\right]. \tag{3}$$

For season h, consider M i.i.d. samples following a known distribution of $(\widetilde{\mathbf{d}}, \widetilde{\mathbf{p}}^{S,h}, \widetilde{\mathbf{p}}^{C,h})$. We index the scenarios by $m \in \mathcal{M} = \{1, \ldots, M\}$ and let $(\mathbf{d}^{h,m}, \mathbf{p}^{S,h,m}, \mathbf{p}^{C,h,m})$ be demand and electricity prices in scenario m, $\forall m \in \mathcal{M}$. Each scenario occurs with probability $q_m^h \geq 0$ such that $\sum_{m\in\mathcal{M}} q_m^h = 1$. The second-stage problem is then equivalent to

$$Q_e^h\left(\mathbf{x}_e^h, \mathbf{z}, \mathbf{s}\right) = \min_{\mathbf{y}^m, \mathbf{w}^m, m\in\mathcal{M}} \sum_{m\in\mathcal{M}} q_m^h \left(\mathbf{c}^{h,m}\right)^{\mathsf{T}}\mathbf{y}^m + \mathbf{g}^{\mathsf{T}}\mathbf{w}^m) \tag{4a}$$

$$\text{s.t.} \quad \left(\mathbf{y}^m, \mathbf{w}^m\right) \in Y\left(\mathbf{x}_e^h, \mathbf{z}, \mathbf{s}, \mathbf{d}^{h,m}\right), \forall m \in \mathcal{M}, \tag{4b}$$

where $\mathbf{c}^{h,m}$ represents the realized cost vector in scenario m under season h. We use $(\mathbf{y}^m, \mathbf{w}^m)$ to denote the recourse solution in scenario m, $\forall m \in \mathcal{M}$.

This approach is known as sample average approximation (Kleywegt et al. 2002, Shapiro and Homem-de-Mello 2000). Kleywegt et al. (2002) provide a sufficient condition for sample size $M \geq 3\sigma_{\max}^2/(\epsilon-\delta)^2 \log(|S|/\alpha)$ where $\delta \in [0, \epsilon)$ and $\epsilon > 0$ is small enough, indicating that an optimal solution obtained by sample average approximation is an ϵ-optimal solution. The significance level $1-\alpha \in (0,1)$ is the probability of the solution calculated from the M samples belonging to the ϵ-optimal set. Set S is the feasible set of integer decision variables, and $\sigma_{\max}^2$ is the maximum variance depending on objective function and the ϵ-optimal solution set. In practice, this bound can be too conservative, and so we choose much smaller sample sizes (described in Section 5.1) to obtain reasonably good solutions.

Recall that $\mathcal{D}_{it}^C \in \mathcal{A}^{\text{charge}}$ is the set of arcs representing EVs being charged in time period t, and $\mathcal{D}_{it}^S \in \mathcal{A}^{\text{sell}}$ is the set of arcs representing EVs in V2G processes in time period t. Let $\delta^+(n_{itb})$ and $\delta^-(n_{itb})$ be the sets of arcs for which n_{itb} is the origin and destination node, respectively. We have

$$\begin{aligned}
&Y\left(\mathbf{x}_e^h, \mathbf{z}, \mathbf{s}, \mathbf{d}^m\right) \\
&:= \{y_a \geq 0, a \in \mathcal{A}, w_{ijts} \geq 0, i,j \in \mathcal{I}_z, s - t \geq l_{ij} :, && \text{(5a)} \\
&\sum_{a\in\delta^+(n_{i1e})} y_a = x_{e,i}^h && \forall i \in \mathcal{I}_z, && \text{(5b)} \\
&\sum_{a\in\delta^+(n_{itb})} y_a - \sum_{a\in\delta^-(n_{itb})} y_a = 0 \\
&\qquad\qquad \forall i \in \mathcal{I}_z,\ t \in \mathcal{T}/\{1,T\},\ b \in \mathcal{B}_e, && && \text{(5c)} \\
&\sum_{a\in\delta^-(n_{iTe})} y_a = x_{e,i}^h && \forall i \in \mathcal{I}_z, && \text{(5d)} \\
&\sum_{a\in\mathcal{D}_{it}^k} y_a \leq u_{\mathcal{D}_{it}^k} && \forall k \in \mathcal{K},\ i \in \mathcal{I}_z,\ t \in \mathcal{T}, && \text{(5e)} \\
&\sum_{a\in\cup_{k\in\mathcal{K}}\mathcal{D}_{it}^k} y_a \leq \sum_{k\in\mathcal{K}} s_i^k && \forall i \in \mathcal{I}_z,\ t \in \mathcal{T}, && \text{(5f)} \\
&\sum_{a\in\mathcal{D}_{ijts}^{\text{rent}}} y_a + w_{ijts} = d_{ijts}^m && \forall i,j \in I_z, t \in \mathcal{T}, s = t + l_{ij}, \ldots, T, \\
&\qquad\qquad && && \text{(5g)} \\
&y_a = 0 && \forall a \in \delta^+(n_{i1b}), b \neq e, b \in \mathcal{B}_e, \\
&\qquad\qquad && \forall a \in \delta^-(n_{iTb}), b \neq B_e, b \in \mathcal{B}_e\}, && \text{(5h)}
\end{aligned}$$

where constraints (5b)–(5d) are flow balance constraints with respect to network $\mathcal{G}$. Constraints (5d) require that the locations of EVs in the last period are reset as their initial locations and all EVs are charged full, for the purpose of operating the carsharing system every T periods with the same initial deployment of fully charged EVs. Constraints (5e) and (5f) are capacity constraints for different types of arcs and parking spaces, respectively. In constraints (5g), w_{ijts} indicates the amounts of unserved demand from zone i to j with starting time t and ending time s. Constraints (5g) also ensure that the total number of EVs being rented out cannot exceed the demand since $w_{ijts} \geq 0$.

Remark 3. Compared with the two-stage model based on a spatial-temporal network in Lu et al. (2018), the complexity of our problem increases due to the introduction of SoC. Suppose that there are N nodes and M arcs in the spatial-temporal network in Lu et al. (2018). Then, the number of nodes in this paper increases to eN and the number of arcs can increase up to e^2M. This inspires us to develop more efficient algorithms in the next section.

4. Solution Approaches

As we relax the second-stage integer variables, the resulting model becomes a two-stage problem with

first-stage integer variables and continuous second-stage variables. Additionally, model (1) can be decomposed into the planning and operational phases, and thus it is natural to apply Benders decomposition to seek optimal solutions by generating optimality cuts from subproblems associated with all the samples. We also explore another algorithm as a scenario decomposition that uses the Lagrangian relaxation method to obtain objective bounds and iteratively applies cutting planes to obtain optimal first-stage solutions that can close the optimality gap. Furthermore, in Online Appendix E for a real-time decision guideline of EV operations, we present a linear-decision-rule-based approximation approach. We describe the details of the first two approaches as follows.

4.1. Benders Decomposition

One classical method to solve two-stage stochastic linear programs is Benders decomposition (Birge and Louveaux 2011), which decomposes the original problem into a relaxed master problem and a set of independent subproblems, one for each scenario $m \in \mathcal{M}$ and each season $h \in \mathcal{H}$. The Benders decomposition approach iteratively generates cuts from each subproblem and adds them to the relaxed master problem if the current first-stage solution is not optimal or feasible. In our model (1), since, for any feasible first-stage solution, we always can find a feasible solution at the operational phase (e.g., having all EVs idle for all T time periods; that is, $y_a = x^h_{e,i}$ for all arcs $a = (n_{ite}, n_{i,t+1,e}) \in \mathcal{A}^{\text{idle}}$ and $y_a = 0$ for all other arcs $a \in \mathcal{A}/\mathcal{A}^{\text{idle}}$), no Benders feasibility cuts are needed and we describe the deviation of the optimality cuts in the following.

We define variables $\theta = (\theta^h_{e,m},\ m \in \mathcal{M}, h \in \mathcal{H}, e \in \mathcal{E})^{\mathrm{T}}$ as lower bounds of $\mathcal{Q}^h_e(\mathbf{x}^h_e, \mathbf{z}, \mathbf{s}, \mathbf{d}^{h,m}, \mathbf{p}^{\mathrm{S},h,m}, \mathbf{p}^{\mathrm{C},h,m})$, $\forall m \in \mathcal{M}$. We formulate the relaxed master problem as

$$\mathbf{MP}: \quad \min_{\mathbf{x},\mathbf{z},\mathbf{s},\sigma,\theta} \sum_{i\in\mathcal{I}}\left(c^{\mathrm{F}}_i z_i + \sum_{k\in\mathcal{K}} c^k_i s^k_i + \sum_{h\in\mathcal{H},e\in\mathcal{E}} c^{\mathrm{V}}_{e,i} x^h_{e,i}\right) + \sum_{e\in\mathcal{E},h\in\mathcal{H}} o_h \sigma_e \sum_{m\in\mathcal{M}} q^h_m \theta^h_{e,m}$$

$$\text{s.t.} \quad L^h_{e,m}(\theta^h_{e,m}, \mathbf{x}^h_e, \mathbf{z}, \mathbf{s}) \geq \mathbf{0},\ \mathbf{m} \in \mathcal{M},\ h \in \mathcal{H},\ e \in \mathcal{E} \qquad (1b)\text{–}(1f),$$

where constraints $L^h_{e,m}(\theta^h_{e,m}, \mathbf{x}^h_e, \mathbf{z}, \mathbf{s}) \geq \mathbf{0}$ denote the set of cuts generated from solving the subproblems in scenario m of season h, which we specify later. To linearize the bilinear terms $\sigma_e\theta^h_{e,m}$ in the objective function, we introduce auxiliary variables $\phi^h_{e,m} = \sigma_e\theta^h_{e,m}$, $h \in \mathcal{H}$, $e \in \mathcal{E}$, $m \in \mathcal{M}$, and McCormick inequalities: $\phi^h_{e,m} \geq \sigma_e\theta^{h,\mathbf{L}}_{e,m} + \theta^h_{e,m} - \theta^{h,\mathbf{L}}_{e,m}$, $\phi^h_{e,m} \leq \sigma_e\theta^{h,\mathbf{U}}_{e,m}$, $\phi^h_{e,m} \leq \theta^h_{e,m} - \theta^{h,\mathbf{L}}_{e,m}(1-\sigma_e)$, $\phi^h_{e,m} \geq \theta^h_{e,m} - \theta^{h,\mathbf{U}}_{e,m}(1-\sigma_e)$, where $\theta^{h,\mathbf{U/L}}_{e,m}$ is the upper/lower bound of $\theta^h_{e,m}$. Alternatively, considering the specific second-stage problem structure, we can drop the coefficient σ_e directly from the objective function and multiply the right-hand side of (5g), d^m_{ijts}, with σ_e, which enforces the second-stage objective value to be 0 when $\sigma_e = 0$. This will result in a different subproblem formulation which can be easily adapted from what we describe below.

Let the dual variables of (5b) and (5d) be π^1_i and π^T_i, respectively. Let α_{itb}, β^k_{it}, γ_{it}, and η_{ijts} be the dual variables associated with constraints (5c), (5e), (5f), and (5g), respectively. For each scenario m of season h, we derive the subproblem dual formulation as

$$\mathbf{SP}\left(\mathbf{x}^h_e, \mathbf{z}, \mathbf{s}, \mathbf{d}^m, \mathbf{p}^{\mathrm{S},h,m}, \mathbf{p}^{\mathrm{C},h,m}\right):$$

$$\max_{\pi^1,\pi^T,\alpha,\beta,\gamma,\eta} \sum_{i\in\mathcal{I}_z}\left(\pi^1_i + \pi^T_i\right)x^h_{e,i} + \sum_{i\in\mathcal{I}_z,k\in\mathcal{K},t\in\mathcal{T}} u_{\mathcal{D}^k_{it}}\beta^k_{it} + \sum_{i\in\mathcal{I}_z,t\in\mathcal{T}}\gamma_{it}\sum_{k\in\mathcal{K}} s^k_i + \sum_{i,j\in\mathcal{I}_z,t,s\in\mathcal{T}} d^{h,m}_{ijts}\eta_{ijts} \qquad (7a)$$

$$\text{s.t.} \quad \pi^1_i - \alpha_{i2e} + \beta^{\mathrm{P}}_{i1} + \gamma_{i1} \leq c^h_a, \quad a = (n_{i1e}, n_{i2e}) \in \mathcal{A}^{\text{idle}} \qquad (7b)$$

$$\pi^1_i - \alpha_{i,2,b'} + \beta^{\mathrm{S}}_{i1} + \gamma_{i1} \leq c^h_a, \quad a = (n_{i1e}, n_{i2b'}) \in \mathcal{A}^{\text{selling}}, b' = e - b^{\mathrm{S}}, \ldots, e-1, \qquad (7c)$$

$$\pi^1_i - \alpha_{jsb} \leq c^h_a,\ 2 \leq s \leq T-1,\ a = (n_{i1e}, n_{jsb}) \in \mathcal{A}^{\text{relo}}, \qquad (7d)$$

$$\pi^1_i - \alpha_{jsb} + \eta_{ij1s} \leq c^h_a,\ 2 \leq s \leq T-1, \quad a = (n_{i1e}, n_{jsb}) \in \mathcal{A}^{\text{rent}}, \qquad (7e)$$

$$\pi^T_i + \alpha_{i,T-1,e} + \beta^{\mathrm{P}}_{i,T-1} + \gamma_{i,T-1} \leq c^h_a, \quad a = (n_{i,T-1,e}, n_{iTe}) \in \mathcal{A}^{\text{idle}}, \qquad (7f)$$

$$\pi^T_i + \alpha_{i,T-1,b'} + \beta^{\mathrm{C}}_{i,T-1} + \gamma_{i,T-1} \leq c^h_a, \quad a = (n_{i,T-1,b'}, n_{iTe}) \in \mathcal{A}^{\text{charge}}, b' = e - b^{\mathrm{C}}, \ldots, e-1, \qquad (7g)$$

$$\alpha_{itb} - \alpha_{i,t+1,b} + \beta^{\mathrm{P}}_{it} + \gamma_{it} \leq c^h_a,\ 2 \leq t \leq T-2, \quad a = (n_{itb}, n_{i,t+1,b}) \in \mathcal{A}^{\text{idle}}, \qquad (7h)$$

$$\alpha_{itb} - \alpha_{i,t+1,b'} + \beta^{\mathrm{C}}_{it} + \gamma_{it} \leq c^h_a, 2 \leq t \leq T-2, \quad a = (n_{itb}, n_{i,t+1,b'}) \in \mathcal{A}^{\text{charge}}, b' = b+1, \ldots, b+b^{\mathrm{C}}, \qquad (7i)$$

$$\alpha_{itb} - \alpha_{i,t+1,b'} + \beta^{\mathrm{S}}_{it} + \gamma_{it} \leq c^h_a, 2 \leq t \leq T-2, \quad a = (n_{itb}, n_{i,t+1,b'}) \in \mathcal{A}^{\text{selling}}, b' = b - b^{\mathrm{S}}, \ldots, b-1, \qquad (7j)$$

$$\alpha_{itb} - \alpha_{jsb'} \leq c^h_a,\ 2 \leq t < s \leq T-1, \quad a = (n_{itb}, n_{jsb'}) \in \mathcal{A}^{\text{relo}}, \qquad (7k)$$

$$\alpha_{itb} - \alpha_{jsb'} + \eta_{ijts} \leq c^h_a,\ 2 \leq t < s \leq T-1, \quad a = (n_{itb}, n_{jsb'}) \in \mathcal{A}^{\text{rent}}, \qquad (7l)$$

$$\eta_{ijts} \le g_{ijts},\ i,j \in \mathcal{I}, 1 \le t < s \le T-1, \text{ such that } d_{ijts} > 0, \tag{7m}$$

$$\beta_{it}^k \le 0,\ \gamma_{it} \le 0,\ i \in \mathcal{I},\ t \in \mathcal{T},\ k \in \mathcal{K}. \tag{7n}$$

At each iteration of the Benders decomposition algorithm, we optimize **MP** to obtain an optimal solution $(\hat{\mathbf{x}}_e^h, \hat{\mathbf{z}}, \hat{\mathbf{s}}, \hat{\theta})$. Then, for each scenario $m \in \mathcal{M}$, we solve the corresponding subproblem $\mathbf{SP}(\hat{\mathbf{x}}_e^h, \hat{\mathbf{z}}, \hat{\mathbf{s}}, \mathbf{d}^{h,m}, \mathbf{p}^{S,h,m}, \mathbf{p}^{C,h,m})$. If the optimal objective value of the subproblem of scenario m is reached and season h is greater than $\hat{\theta}_{e,m}^h$ given by **MP** and an optimality cut is generated and added to $L_{e,m}^h(\theta_{e,m}^h, \mathbf{x}_e^h, \mathbf{z}, \mathbf{s}) \ge \mathbf{0}$ in the current **MP**. Given an optimal solution $(\hat{\pi}^1, \hat{\pi}^T, \hat{\alpha}, \hat{\beta}, \hat{\gamma}, \hat{\eta})$ to the subproblem $\mathbf{SP}(\hat{\mathbf{x}}_e^h, \hat{\mathbf{z}}, \hat{\mathbf{s}}, \mathbf{d}^{h,m}, \mathbf{p}^{S,h,m}, \mathbf{p}^{C,h,m})$, following strong duality, a Benders cut takes the following form:

$$\theta_{e,m}^h - \sum_{e\in,i\in\mathcal{I}_z} \left(\hat{\pi}_i^1 + \hat{\pi}_i^T\right) x_{e,i}^h - \sum_{i\in\mathcal{I},k\in\mathcal{K},t\in\mathcal{T}} u_{\mathcal{D}_{it}^k} \hat{\beta}_{it}^k - \sum_{i\in\mathcal{I},t\in\mathcal{T}} \hat{\gamma}_{it} \sum_{k\in\mathcal{K}} s_i^k - \sum_{i,j\in\mathcal{I},t,s\in\mathcal{T}} d_{ijts}^{h,m} \hat{\eta}_{ijts} \ge 0. \tag{8}$$

4.2. Scenario Decomposition

Alternatively, we consider a scenario decomposition approach for optimizing model (1). We further assume that $q_m^1 = \cdots = q_m^{|\mathcal{H}|} = 1/M$ for $m \in \mathcal{M}$. We separate first-stage decision variables into $(1+H)|\mathcal{E}|$ vectors: $\mathbf{x}_e^h$, $h \in \mathcal{H}$, $e \in \mathcal{E}$, and $\mathbf{X} = (\mathbf{z}, \mathbf{s}, \sigma)$. We denote $\boldsymbol{C}_x^{h,e}$ and $\mathbf{C}_X$ as the cost vectors of $\mathbf{x}_e^h$, $h \in \mathcal{H}$, $e \in \mathcal{E}$ and $\mathbf{X}$, respectively. Let $\mathcal{X}_e^h = \{\mathbf{x}_e^h : (1d)\text{--}(1f)\}$ and $\mathcal{X} = \{\mathbf{X} = (\mathbf{z}, \mathbf{s}, \sigma) : (1b), (1c), (1f)\}$ be the feasible region defined by all the first-stage constraints. We also denote $\mathbf{Y}_m^{h,e} = (\mathbf{y}_m^{h,e}, \mathbf{w}_m^{h,e})$ as the recourse decision in scenario m of season h under battery capacity e, and we denote $\mathbf{C}_{Y,m}^{h,e}$ as the cost vector of $\mathbf{Y}_m^{h,e}$. For each season $h \in \mathcal{H}$ with battery capacity e, we make M copies of vector $\mathbf{x}_e^h$ for each scenario, denoted by $\mathbf{x}_{e,m}^h$, $\forall m \in \mathcal{M}$, such that

$$\mathbf{x}_{e,1}^h = \cdots = \mathbf{x}_{e,M}^h. \tag{9}$$

We also make copies of vector $\mathbf{X}$ for each scenario, denoted by $\mathbf{X}_m$, $\forall m \in \mathcal{M}$, such that

$$\mathbf{X}_1 = \cdots = \mathbf{X}_M. \tag{10}$$

Theorem 1. *For a scenario $m \in \mathcal{M}$, given parameters μ and $\boldsymbol{\lambda} = (\lambda^{h,e}, h \in \mathcal{H}, e \in \mathcal{E})$, consider a Lagrangian function*

$$\mathcal{L}_m(\boldsymbol{\lambda}, \mu) = \min_{\mathbf{x}_{e,m}^h, \mathbf{X}_m, \mathbf{Y}_m^{h,e}} \left\{ q_m \left[\mathbf{C}_X^\top \mathbf{X}_m + \sum_{h\in\mathcal{H},e\in\mathcal{E}} o_h \left(\left(\mathbf{C}_x^{h,e}\right)^\top \mathbf{x}_{e,m}^h + \left(\mathbf{C}_{Y,m}^{h,e}\right)^\top \mathbf{Y}_m^{h,e} + \left(\lambda^{h,e}\right)^\top A_{x,m}^{h,e} \mathbf{x}_{e,m}^h \right) \right] + \mu^\top A_m \mathbf{X}_m : \mathbf{x}_{e,m}^h \in \mathcal{X}_e^h, \mathbf{X}_m \in \mathcal{X}, \mathbf{Y}_m^{h,e} \in Y\left(\mathbf{x}_{e,m}^h, \mathbf{X}_m, \mathbf{d}^{h,m}\right) \right\}. \tag{11}$$

An optimal solution to the problem $\max_{\lambda^{h,e},\mu} \sum_{m\in\mathcal{M}} \mathcal{L}_m(\boldsymbol{\lambda}, \mu)$ provides a valid lower bound for model (1).

The details of the proof can be found in Online Appendix C. In (2b), noting that the objective function and constraints in the minimization problem are decomposable by scenario, we can first optimize scenario-based subproblems (11) and then aggregate the results to obtain a lower bound for any given $\boldsymbol{\lambda}$ and μ.

For given $\boldsymbol{\lambda}$ and μ, suppose that solution $(\mathbf{x}_{e,m}^{h,*}, \mathbf{X}_m^*)$ optimizes the above m-scenario-based subproblem (11) and yields an optimal objective value $\mathbf{OBJ}^{m,*}$. We obtain a lower bound $\mathrm{LB} = \sum_{m\in\mathcal{M}} \mathbf{OBJ}^{m,*}$. We can apply the subgradient method to update $\boldsymbol{\lambda}$ and μ to strengthen LB. On the other hand, any $(\mathbf{x}_{e,m}^{h,*}, \mathbf{X}_m^*)$ is a feasible solution to the original problem (1), and therefore a feasible upper bound $\mathrm{UB} = \mathbf{C}_X^\top \mathbf{X}_m^{h,*} + \sum_{h\in\mathcal{H}} o_h \times [(\mathbf{C}_x^{h,e})^\top \mathbf{x}_{e,m}^{h,*} + \sum_{n\in\mathcal{M}} q_n \mathcal{Q}_e^h(\mathbf{x}_{e,m}^{h,*}, \mathbf{X}_m^*, \mathbf{d}^{h,n}, \mathbf{p}^{S,h,n}, \mathbf{p}^{C,h,n})]$. The best upper bound is obtained as

$$\min_{m\in\mathcal{M}} \left\{ \mathbf{C}_X^\top \mathbf{X}_m^{h,*} + \sum_{h\in\mathcal{H}} o_h \left[\left(\mathbf{C}_x^{h,e}\right)^\top \mathbf{x}_{e,m}^{h,*} + \sum_{n\in\mathcal{M}} q_n \mathcal{Q}_e^h\left(\mathbf{x}_{e,m}^{h,*}, \mathbf{X}_m^*, \mathbf{d}^{h,n}, \mathbf{p}^{S,h,n}, \mathbf{p}^{C,h,n}\right) \right] \right\}. \tag{12}$$

We use binary representation of the general integer variables, specifically, the $\mathbf{x}$- and $\mathbf{X}$-variables. If $\mathrm{UB} > \mathrm{LB}$, then we prohibit such solutions from being generated in future iterations by adding no-good cuts for binary variables in all subproblems (11). We iterate the above process until $\mathrm{UB} \le \mathrm{LB}$ for some optimal solution $(\mathbf{x}_{e,m}^{h,*}, \mathbf{X}_m^{h,*})$, which will automatically satisfy the nonanticipativity constraints and be returned as the overall optimal solution for $(\mathbf{x}_e^h, \mathbf{X})$. Note that since $(\mathbf{x}_e^h, \mathbf{X})$ is integral, we have only a finite number of possible first-stage solutions to cut, and therefore the algorithm terminates in finite steps.

5. Computational Results

In this section, we use Zipcar's carsharing demand data in the Boston–Cambridge, Massachusetts, area in 2014 (following data descriptions in Lu et al. 2018) and synthetic data to generate diverse instances with various carsharing demand types, spatial-temporal patterns, seasonal electricity buying and selling prices, battery degradation costs, battery capacities, and charging speeds. We test our two-stage optimization model and solution algorithms on these instances to demonstrate the computational efficiency of the algorithms and draw insights on the benefit of integrating V2G into EV sharing.

5.1. Experimental Design and Setup

We mainly follow Lu et al. (2018) and Chang et al. (2017) to generate all instances and consider five

potential service zones in our studies. We let each operational time period be 15 minutes, and we repeatedly operate the system on a daily basis. Therefore, the planning horizon T is 24 hours or, equivalently, 96 time periods. We set the maximum number of the three types of parking spaces (i.e., P–parking only, C–parking space with charging stations, and S–parking space with bidirectional charging stations) as 300, 100, and 100 for all service zones.

We scale all the planning cost parameters (i.e., c_i^{F}, $c_{e,i}^{\mathrm{V}}$, and c_i^k) to cost per day. Following cost justification as in Lu et al. (2018), we set $c_i^{\mathrm{F}} = \$9.60$ per parking lot per day for all zones. The idle cost c_i^{idle} is \$0.10 per period, and the cost of relocating one EV c_{ij}^{relo} is \$2.50 per period in-between any pairs of zones i and j. In addition to the fixed cost c_i^{F}, we consider the costs of equipping a parking lot to become P-, C-, and S-types of parking spaces, and we set them as $c_i^{\mathrm{P}} = \$0.00$, $c_i^{\mathrm{C}} = \$0.70$, and $c_i^{\mathrm{S}} = \$5.50$ per parking lot per day, for all zones i. The latter two costs are calculated by assuming that the prices of regular and bidirectional charging stations are \$1,200 and \$10,000, respectively, and that the average lifetime of each charging station is five years.[3]

In the baseline model, the battery capacity is $e = 20$ kWh or 20 SoC units, which is a typical EV battery capacity. The cost of locating one EV in any service zone is $c_{e,i}^{\mathrm{V}} = \$27.00$ per vehicle per day, calculated based on EV purchase price and average maintenance cost. We consider both *regular charging* of rate 1 SoC unit/period (i.e., 4 kW) and *fast charging* of rate 10 SoC units/period (i.e., 40 kW). The battery discharge rate is 2 SoC units/period for driving (i.e., 8 kW), and is 4 SoC units/period for V2G selling (i.e., 16 kW). We assume that there is no degradation cost associated with either charging or V2G procedures in the baseline model, and we will study the impact of various degradation costs in a later computational test.

We use three months of Zipcar 2014 data in the Boston–Cambridge area to generate rental demand. The original data set contains both one-way and round-trip rentals. Unfortunately, the actual driving time of round trips was not recorded in the data set, making it impossible to estimate the battery discharge associated with each trip. Therefore, we focus on one-way trips. Following Lu et al. (2018) and Chang et al. (2017), demand per period follows the gamma distribution, with hourly average demand shown in Figure 3. Based on the Zipcar 2014 data, we generate a one-way travel time from a uniform distribution between 15 to 45 minutes. We use the actual rental rate charged by Zipcar to its one-way rental services, that is, $r_{ij} = \$3.00$ per period or \$12.00 per hour. In the baseline case, we consider the unit penalty cost of not fulfilling a trip the same as its revenue.

We assume uncertain electricity prices of regular charging and fast charging. For the following computational studies, we assume that the V2G price is the same as the charging price. In Online Appendix G, we present the results by assuming a fixed-price V2G contract with a time-of-use (ToU) type. Given that the V2G technology is in the early stage of commercial adoption, its market value is still uncertain. The two cases considered here are conservative. Under higher selling prices, the value of V2G integration may be even higher. We follow real-world data to set electricity prices for charging and V2G selling, and we differentiate the prices for winter and summer time. (More details about electricity prices are given in Online Appendix D.)

All of the computational tests are performed on a Windows Server 2012 R2 Standard with Intel(R) Xeon(R) CPU E5-2630 v4 CPU 2.20 GHz, 20 cores (40 logical processors), and 128 GB memory. We implement all the computation tests in Python with Gurobi 8.0.1 as the optimization solver.

5.2. Computational Study

We first solve the two-stage model (1) with integer recourse variables and compare the objective values with those from solving relaxation models with continuous recourse variables. In Table 2, we present the objective values and CPU time of five instances solved with continuous and integer recourse. The CPU time in seconds is reported for both models. We note that all the integer recourse models failed to be solved within 32 hours (= 115,200 seconds). The optimality gaps (opt. gap) of the integer recourse are reported, and their objective values provide upper bounds (UB) of the true optimal. The objective values of the relaxation models with continuous recourse are the lower bounds (LB) of the true optimal. The relative difference (rel. diff.) is calculated as $(\mathrm{UB} - \mathrm{LB})/\mathrm{UB} \times 100\%$, the ratio of the difference of two objectives to the objective of integer recourse.

Figure 3. (Color online) Hourly Demand Pattern in the Zipcar 2014 Data in the Boston–Cambridge Area Reported in Chang et al. (2017)

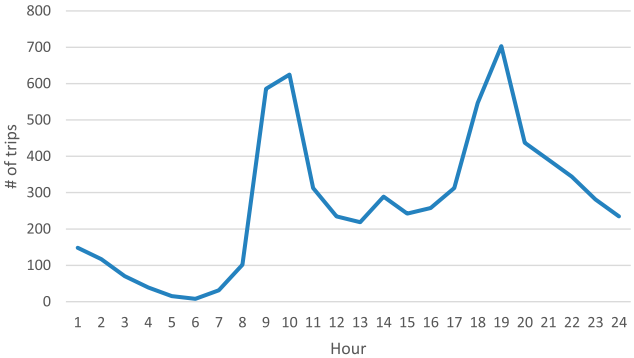

Table 2. Objective and CPU Time Comparison Between Models With Integer and Continuous Recourse Variables

Recourse type	Continuous			Integer		
Instance	Rel. diff. (%)	LB	Time (s)	UB	Opt. gap (%)	Time (s)
1	0.13	–1,418.59	3,228	–1,416.74	0.21	Limit
2	0.85	694.35	3,649	700.29	0.95	Limit
3	0.23	957.48	2,914	959.65	0.25	Limit
4	5.13	159.88	3,203	168.52	5.33	Limit
5	1.11	687.04	3,029	694.77	1.19	Limit

Note. Rel. dif., relative difference; LB, lower bound; UB, upper bound; opt. gap, optimality gaps.

Among the first three instances, the objective values of continuous recourse are less than those of integer recourse variables, and their relative differences are less than 1%. For the last two instances having larger optimality gaps when solved with integer recourse, all the relative differences are within their corresponding optimality gaps. Therefore, in the following tests we relax the integrality constraints on recourse variables.

Next, we compare the computational time of the three solution approaches based on the relaxation model with continuous recourse variables: approach (i) directly solving the MILP model (1) using Gurobi, Approach (ii) Benders decomposition in Section 4.1, and approach (iii) scenario decomposition in Section 4.2. The two decomposition algorithms are parallelly implemented via ThreadPoolExecutor of the concurrent.futures module in Python. All subproblems (7), (11), and (12) are solved in parallel. The results demonstrate the efficiency of our tailored solution methods [i.e., methods (ii) and (iii)] when compared with the off-the-shelf commercial solvers. Following Lu et al. (2018), in each instance, we consider nine service zones (into which the Boston–Cambridge area is divided) and 50 scenarios of uncertainties (i.e., electricity prices and rental demand). The electricity prices are randomly generated from a normal distribution, with mean and standard deviation calculated from the real-world price data. The rental demand scenarios are generated following the procedure described in Section 5.1.

Table 3 shows the total CPU time (see columns "Overall") taken by all three approaches, as well as the average time of solving the master problems (see column "MP") and subproblems (see column "SP") by Benders decomposition, as well as the average time of solving subproblems (11) to obtain a valid lower bound (reported under column "LB") and calculating upper bound (12) (reported under column "UB") by scenario decomposition. The time limit in this test is set at 8 hours (= 28,800 seconds).

In Table 3, for all the instances, directly solving the MILP model takes a significantly longer time, as compared with the other two decomposition algorithms. The scenario decomposition slightly outperforms the Benders decomposition with an average solution time of 276.60 seconds. The Benders decomposition spends most of the time in solving dual-based subproblems to obtain Benders cuts. The scenario decomposition approach spends most of the time on solving the scenario-based subproblems (11).

In practice, it may sometimes be necessary to solve instances with larger sizes compared with those in Table 3. To tackle these situations, the decomposition methods can be implemented parallelly using message passing interfaces such as Open MPI[5] to further improve the CPU time.[4] In addition, the SoC levels and time periods can be grouped, and thus the

Table 3. CPU Time (in Seconds) Comparison of Solving MILP, Benders, and Scenario Decomposition

	MILP	Benders decomposition			Scenario decomposition		
Instance	Overall	Overall	MP	SP	Overall	LB	UB
1	3,502.17	85.78	4.67	81.11	464.44	309.18	155.26
2	Limit	675.27	286.28	388.99	262.10	158.43	103.66
3	13,725.71	168.55	14.35	154.19	261.39	186.45	74.94
4	Limit	871.75	364.55	507.20	242.00	153.19	88.82
5	852.95	168.53	18.29	150.24	153.07	82.88	70.19
Average	15,136.17	393.98	137.63	256.35	276.60	178.03	98.57

Note. MP, master problem; SP, subproblem; LB, lower bound; UB, upper bound.

Table 4. The Benefit of V2G Integration and the Impact of Fast Charging and Seasonality

V2G		Yes		No		Yes		No	
Fast charge		Yes		Yes		No		No	
Total profit ($)		3,664.30		2,941.25		3,081.88		2,153.49	
% increase		24.58		N/A		43.11		N/A	
Season		Winter	Summer	Winter	Summer	Winter	Summer	Winter	Summer
EVs deployed		197	211	184	188	231	233	218	216
Service level (%)		91	92	90	89	86	86	83	83
V2G amount (kWh)		2,863.04	2,595.47	N/A	N/A	3,826.23	3,198.12	N/A	N/A
Revenue ($)	Rental	5,729.10	5,756.50	5,645.74	5,622.66	5,332.51	5,349.30	5,208.52	5,187.81
	V2G	175.94	814.13	N/A	N/A	228.38	936.88	N/A	N/A
Cost ($)	Relocation	552.50	551.79	530.63	517.48	474.50	480.38	436.20	430.60
	Idle	7.87	85.78	342.25	353.14	9.35	97.73	462.30	455.55
	Charging	598.50	1,015.63	496.20	880.25	347.42	558.40	148.20	259.47
Charging (kWh)	Regular	6,181.51	6,130.63	3,093.82	3,192.28	7,760.83	7,148.62	3,821.31	3,803.02
	Fast	942.94	743.94	1,094.51	970.14	N/A	N/A	N/A	N/A
	Net total	4,261.40	4,279.10	4,188.33	4,162.43	3,934.60	3,950.50	3,821.31	3,803.02
	% increase	1.74	2.80	N/A	N/A	2.96	3.88	N/A	N/A

number of second-stage variables can be reduced. An alternative approximation method (presented in Online Appendix E) can also be considered to improve computational efficiency.

5.3. Benefit of V2G Integration

We now study various benefits of integrating V2G in EV sharing, as well as how the benefits are impacted by important factors such as battery degradation costs, fast charging technology, seasonality of demand and electricity price, and urban spatial structure.

We consider four performance measures, including the total operating profit [the negative of the objective value in (1a) excluding the penalty cost for unserved demand], service level (the percentage of rental requests that are fulfilled in both summer and winter time), the number of deployed EVs (in both summer and winter), and the amount of electricity sold to the grid (in summer and winter). Among these performance measures, the operating profit represents the benefit to carsharing service providers; the service level represents the benefit to consumers, that is, carsharing users. According to recent studies, each vehicle added to a carsharing fleet can replace up to 15 private vehicles, which correspond to more than 100,000 private car miles per year (Glotz-Richter 2016). Therefore, the number of deployed EVs reflects the socioenvironmental benefit. The amount of V2G electricity represents the benefit to the power grid.

Table 5. The Benefit of V2G Integration Under Higher Service Penalty and Longer Travel Time

		Baseline scenario		High service requirement		Long travel time	
V2G		Yes	No	Yes	No	Yes	No
Total profit ($)		3,664.30	2,941.25	3,407.45	2,493.50	4,788.82	3,678.56
% increase		24.58	N/A	36.65	N/A	30.18	N/A
Service level (%)		91.39	89.27	93.58	92.51	93.07	91.20
EVs deployed	Winter	197	184	214	207	289	273
	Summer	211	188	230	211	307	281
V2G amount (kWh)		5,458.51	N/A	6,313.37	N/A	7,996.68	N/A
Revenue ($)	Rental	11,485.60	11,268.40	11,682.00	11,584.88	18,038.12	17,792.18
	V2G	990.07	N/A	1119.72	N/A	1545.98	N/A
Cost ($)	Relocation	1,104.29	1,048.11	1,165.00	1,149.38	2,205.55	2,135.57
	Idle	93.65	695.39	99.23	831.50	105.71	1,022.85
	Charging	1,614.13	1,376.45	1,602.63	1,267.61	3,698.22	3,228.00
Charging (kWh)	Regular	12,312.13	6,286.10	13,662.39	6,999.04	17,500.76	8,743.69
	Fast	1,686.88	2,064.65	1,370.98	1,643.71	4,285.76	4,826.22
	Net total	8,540.50	8,350.76	8,720.00	8,642.75	13,789.85	13,569.91
	% increase	2.27	N/A	0.89	N/A	1.62	N/A

Table 6. The Benefit of V2G Integration With Various Battery Degradation Costs

Degradation cost ($/kWh)		0		0.01		0.05	
V2G		Yes	No	Yes	No	Yes	No
Total profit ($)		3,664.30	2,941.25	3,338.03	2,677.20	2,152.87	1,730.00
% increase		24.58	N/A	24.68	N/A	24.44	N/A
Service level (%)		91.39	89.27	91.27	89.17	90.21	89.08
EVs deployed	Winter	197.00	184.00	200.00	186.00	208.00	203.00
	Summer	211.00	188.00	213.00	191.00	224.00	209.00
V2G amount (kWh)		5458.51	N/A	5470.42	N/A	5325.60	N/A
Revenue ($)	Rental	11,485.60	11,268.40	11,483.59	11,269.72	11,418.41	11,310.04
	V2G	990.07	N/A	944.74	N/A	715.88	N/A
Cost ($)	Relocation	1,104.29	1,048.11	1,093.13	1,039.23	1,040.32	1,009.22
	Idle	93.65	695.39	100.43	708.84	163.87	815.56
	Charging	1,614.13	1,376.45	1,831.95	1,567.65	2,457.83	1,994.06
Charging (kWh)	Regular	12,312.13	6,286.10	12,424.15	6,408.36	12,660.42	7,064.92
	Fast	1,686.88	2,064.65	1,576.50	1,936.17	1,109.71	1,282.48
	Net total	8,540.50	8,350.76	8,530.23	8,344.53	8,444.53	8,347.40
	% increase	2.27	N/A	2.23%	N/A	1.16	N/A

5.3.1. Impact of Fast Charging and Seasonality. Table 4 shows the performance measures along with detailed results of revenue, cost, and charging operations, with or without V2G procedures and with or without fast charging technology in winter and summer time. The fourth row, "% increase," is the percentage of profit increase with V2G compared with the case without V2G procedure. Similarly, the last row "% increase" shows the percentage of net total charging increase compared with the case without V2G.

We have several observations from Table 4.

- First, integrating V2G in EV sharing can significantly increase profitability. The benefit of V2G is more significant when fast charging is not available. Both V2G and fast charging can improve the service level. The combination of V2G and fast charging can achieve significant improvement in both profitability and quality of service.
- Second, the integration of V2G technology significantly increases the size of the EV fleet, whereas the use of fast charging decreases the fleet size. For example, implementing V2G alone can increase the fleet size by an average of 15, whereas fast charging along can reduce the fleet size by an average of 31. Recall that studies have shown that each EV added to the carshare fleet can replace up to 15 private cars (Bondorová and Archer 2017), which is the major socioenvironmental benefit of EV sharing.

Table 7. The Benefit of V2G Integration With Battery Capacity Choices

V2G		Yes		No	
Battery capacity		30		20	
Total profit ($)		3,707.17		2,941.25	
% increase		26.04		N/A	
Service level (%)		91.85		89.27	
Season		Winter	Summer	Winter	Summer
EVs deployed		195	225	184	188
Service level (%)		90.94	92.76	89.63	88.91
V2G amount (kWh)		2,651.02	3,105.42	N/A	N/A
Revenue ($)	Rental	6,005.81	6,100.41	5,645.74	5,622.66
	V2G	185.25	1,218.27	N/A	N/A
Cost ($)	Relocation	572.34	586.02	530.63	517.48
	Idle	3.35	35.57	342.25	353.14
	Charging	633.37	1,553.93	496.20	880.25
Charging (kWh)	Regular	6,007.96	6,927.64	3,093.82	3,192.28
	Fast	1,104.81	1,104.81	1,094.51	970.14
	Net total	4,461.75	4,927.03	4,188.33	4,162.43
	% increase	6.53%	18.37%	N/A	N/A

Table 8. The Benefit of V2G Integration Under Different Urban Spatial Structures

Spatial structure		Random		Concentrated		CRDB		DRCB	
V2G		Yes	No	Yes	No	Yes	No	Yes	No
Total profit ($)		3,664.30	2,941.25	1,765.86	1,071.88	1,181.69	709.51	1,311.02	642.95
% increase		24.58	N/A	64.74	N/A	66.55	N/A	103.91	N/A
Service level (%)		91.39	89.27	91.01	88.00	88.51	82.15	87.53	83.46
EVs deployed	Winter	197	184	183	165	179	150	194	173
	Summer	211	188	205	176	190	147	212	178
V2G amount (kWh)		5,458.51	N/A	5,722.49	N/A	6,041.63	N/A	6,169.46	N/A
Revenue ($)	Rental	11,485.60	11,268.40	10,075.14	9,839.69	9,533.40	8,983.48	10,155.73	9,806.44
	V2G	990.07	N/A	1,026.07	N/A	1,037.13	N/A	1,086.12	N/A
Cost ($)	Relocation	1,104.29	1,048.11	1,505.77	1,562.86	1,546.48	1,493.13	1,586.94	1,583.25
	Idle	93.65	695.39	107.22	688.91	91.08	647.02	149.06	772.56
	Charging	1,614.13	1,376.45	1,884.96	1,668.53	2,161.08	1,935.62	2,108.74	1,839.17
Charging (kWh)	Regular	12,312.13	6,286.10	11,411.54	5,086.33	10,676.05	3,662.77	11,516.11	4,688.29
	Fast	1,686.88	2,064.65	2,232.33	2,723.75	2,958.37	3,520.72	2,693.38	3,115.93
	Net total	8,540.50	8,350.76	7,921.38	7,810.08	7,592.79	7,183.49	8,040.03	7,804.23
	% increase	2.27	N/A	1.43	N/A	5.70	N/A	3.02	N/A

Note. CRDB, centralized residential and distributed business; DRCB, distributed residential and centralized business.

- Third, V2G selling can provide substantial flexible electricity back to the grid. Considering the net total electricity consumption, which is the sum of regular and fast charging minus V2G, the integration of V2G only causes a very minimal increase in the net total electricity while generating benefits in multiple aspects.

5.3.2. Impact of Higher Service Penalty and Longer Travel Time. As the carsharing industry becomes increasingly competitive, it is important for service providers to maintain high levels of service quality, especially in large cities with excessive traffic congestion. Therefore, we study the benefit of V2G selling under higher service requirements and longer travel times. For service requirements, we double the penalty cost of unmet demand to be twice the revenue of the unfulfilled rental request. For travel time, we also double the average trip time. The result details are shown in Table 5.

In Table 5, compared with the baseline case, V2G selling leads to more significant improvement in profitability under higher service penalty or longer travel time. The amount of V2G electricity is also larger under higher service penalty or longer travel time, as more EVs are being deployed.

5.3.3. Impact of Battery Degradation. EV manufacturers have debated over whether battery degradation may hinder the effectiveness of V2G, making it economically infeasible. For example, Tesla originally objected to the idea of V2G, citing battery degradation as the major concern, but recently announced that it might reconsider the possibility. Nissan, on the other hand, has always maintained that battery degradation will not affect V2G operations (Lambert 2018). The cost of battery degradation depends on the battery purchase cost and battery lifetime degradation from charging/discharging. We follow Peterson et al. (2010) and assume that the battery degradation cost is proportional to the SoC unit changes from charging/discharging.

To study the impact of battery degradation, we vary the unit degradation cost from 0.0 to 0.05 $/kWh based on the calculations in Peterson et al. (2010) and present the results in Table 6. We see that battery degradation may worsen system performance regarding profitability and quality of service, with or without V2G. However, given the same battery degradation cost, V2G integration can still significantly benefit EV sharing systems, resulting in higher profit, better service, and a larger fleet. Compared with the baseline case with no degradation cost, the increase in profit from V2G integration is similar with battery degradation cost. The fast charging amount decreases greatly under higher degradation costs, which may be a result of the increase in fast charging prices due to the degradation costs. These results suggest that V2G integration is beneficial, despite battery degradation, and its benefit may be more or less as the degradation cost increases.

5.3.4. Impact of V2G on the Service Provider's Choice of Battery Capacity. There are various EVs with different battery capacities in the current market, such as the Nissan LEAF with a 30-kWh battery pack, the Ford Focus Electric with a 33-kWh battery pack, and the Hyundai Ioniq Electric with a 28-kWh battery pack. Different choices of battery capacities can impact the rental, charging, V2G, and vehicle repositioning operations. Furthermore, because the "range anxiety" is a major concern in EV adoption (see, e.g., Lim et al. 2014), an EV fleet with larger batteries (i.e., longer ranges) can attract more users. Therefore, study

Figure 4. Hourly Numbers of Idle EVs at Each Zone Under Different Spatial Structures

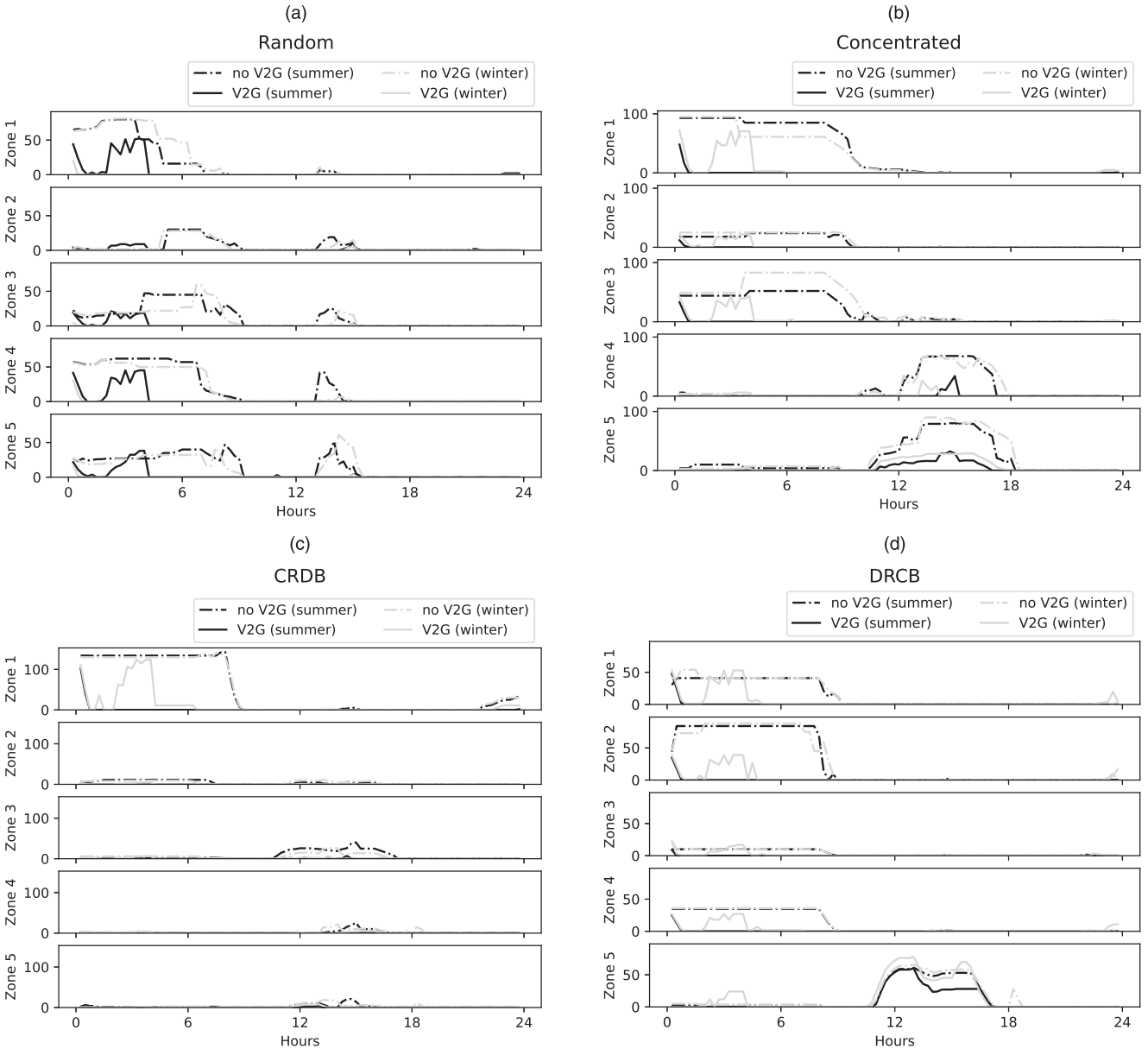

how V2G integration may affect the service provider's choice of battery capacity. We consider two battery capacity options: 20 kWh and 30 kWh. The cost of locating one EV with 20 kWh is \$27.00 and is \$27.50 with 30 kWh. The solution details with and without V2G procedures are shown in Table 7.

In Table 7, when the V2G procedure is available, the larger battery capacity 30 kWh is selected; but the smaller battery is preferred without V2G. Therefore, V2G integration induces the service provider to deploy EVs with larger batteries and longer ranges, which may in turn facilitate the adoption of EV sharing. Similar to our previous observations, with battery capacity choices, V2G still leads to various benefits, including higher profitability, better service, and larger fleet size.

5.4. Impact of Urban Spatial Structure

Next, we look into the impact of urban spatial structure, that is, the pattern of residential and business/commercial land use in urban areas. The relative location of residential and business areas largely determines the traffic pattern during morning and evening rush hours. Based on the Zipcar 2014 data, the majority (approximately 90%) of the trips are from residential sectors to business districts in the morning (9 a.m. to 11 a.m.) and in the reverse direction during the evening (5 p.m. to 10 p.m.). The rush hours are identified by the hourly demand shown in Figure 3.

In the following study, depending on the major function of each zone, we consider four different spatial distributions of demand, which affects the

Figure 5. Hourly Numbers of Unmet Demand at Each Zone Under Different Spatial Structures

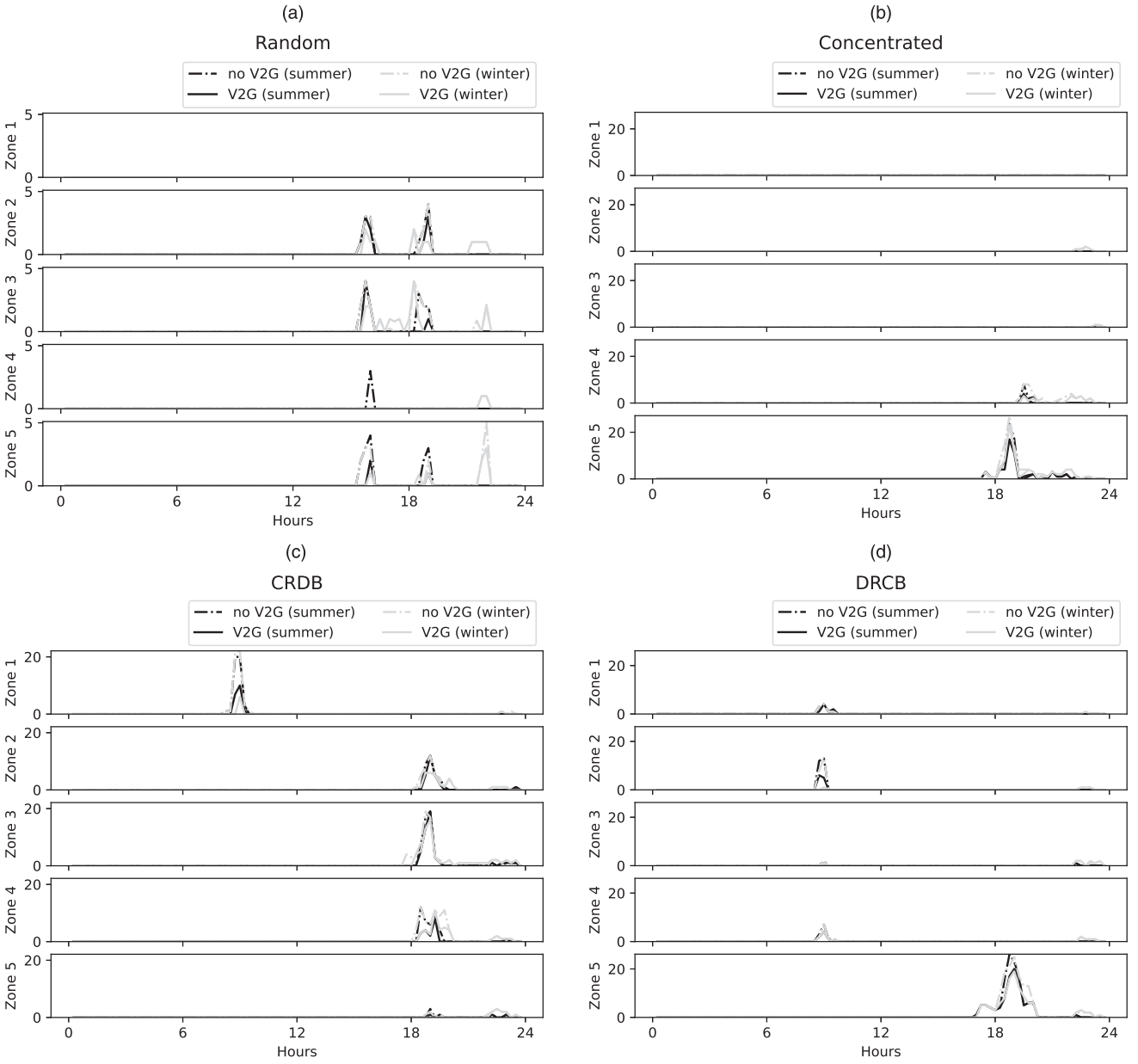

distribution of rental requests but not the geographical relations or travel times.

1. *Random*: a city where residential and business land use is geographically dispersed. Carsharing demands are randomly distributed and do not have any specific spatial pattern. This is the structure that we use in the baseline case in all the previous sections.

2. *Concentrated*: a city where residential sectors (zones 1, 2, and 3 in our numerical study) and business districts (zones 4 and 5) are separated.

3. *Centralized residential and distributed business (CRDB)*: a city with a centralized residential zone (zone 1) and multiple business districts in zones 2, 3, 4, and 5.

4. *Distributed residential and centralized business (DRCB)*: a city with multiple residential sectors in zones 1, 2, 3, and 4, and a centralized business district (zone 5).

Table 8 shows the solution details under different spatial structures. (We focus on the case with fast charging options.) The observations from Section 5.3 still hold. That is, with V2G procedures available, the operating profit increases greatly, the quality of service is improved, and more EVs are deployed, under all considered spatial structures. Compared with the random structure case, V2G selling has a more significant impact on improving profitability with concentrated residential/business areas.

Figure 6. Hourly Numbers of EVs Charged and in V2G Procedures at Each Zone Under the Random Structure

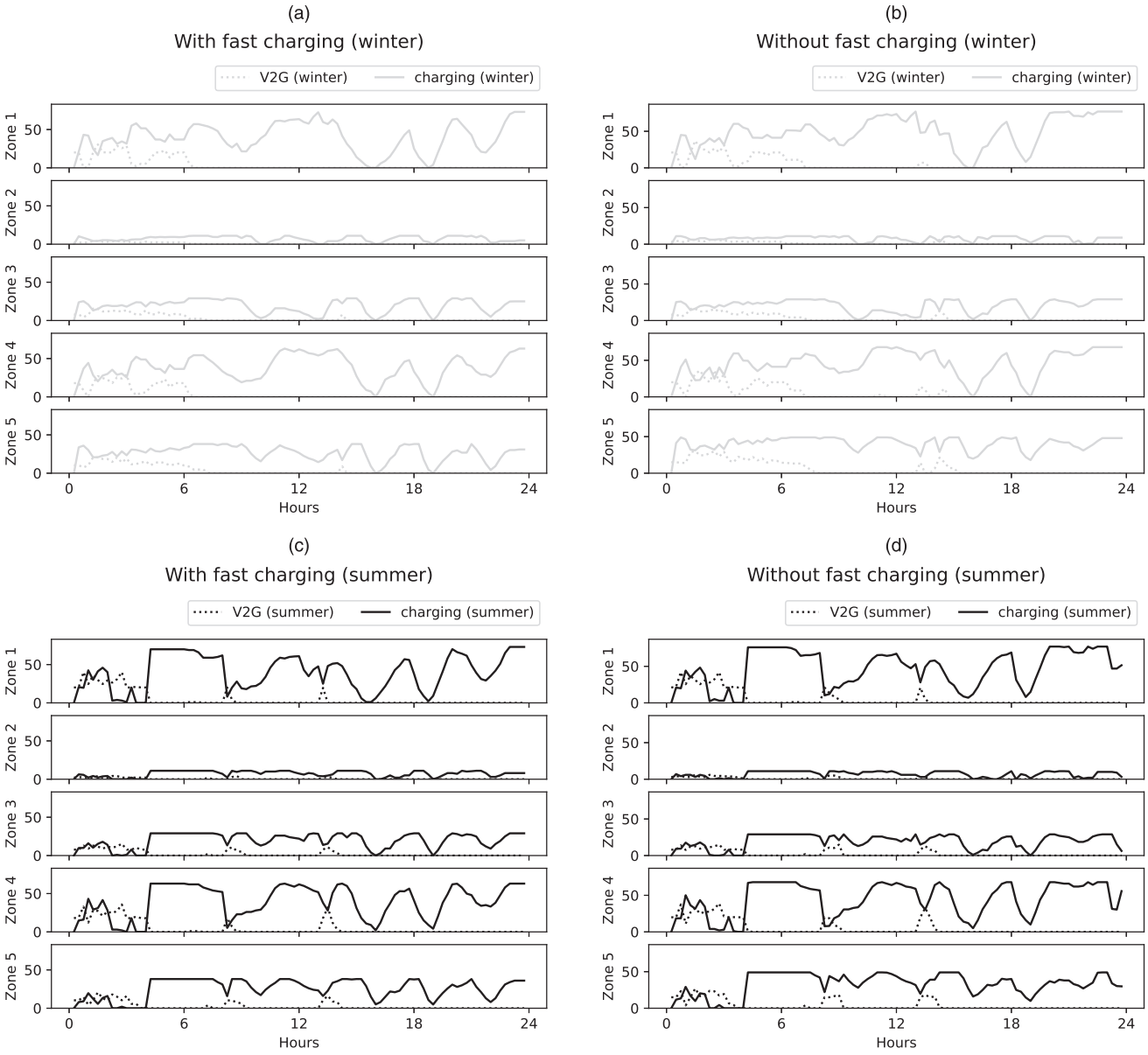

5.5. Hourly Operational Patterns

So far, we have focused on aggregate performance measures. In this section, we look into the hourly patterns of vehicle movement and charging operations to gain more insights. We present the second-stage decision variables under one randomly selected scenario in the two-stage stochastic programming model. The hourly rental demand is presented in Online Appendix F.

Figure 4 demonstrates the numbers of idle EVs with/without V2G procedures. In all of the cases, most of the time, the total number of idle EVs with V2G available is much lower than those without V2G. Under the random structure, the plots at different zones have similar patterns. When V2G is not available, most EVs are idle before the morning rush hours and before the evening rush hours. When V2G is available, EVs are only idle in the morning before the rush hours. Under the other three spatial structures, the patterns vary, depending on whether the zone is a residential area or a business district. In the residential areas, most idle EVs appear in the morning, while in the business areas, most are before the evening rush hours. For example, in Figure 4(b), zones 1–3 are residential areas, where most idle EVs appear in the morning. Whereas, in zones 4 and 5, the majority appears during the afternoon.

Figure 5 demonstrates the hourly numbers of unmet demand with/without V2G procedures. The unmet demand patterns with and without V2G procedures are very similar. With V2G, the amount of

unmet demand has more reduction in the residential areas compared with the business areas such as under "Concentrated," "CRDB," and "DRCB" structures.

Figure 6 shows the numbers of EVs being charged and the numbers of EVs in V2G processes under the random spatial structure. We consider the recourse solutions of winter and summer time, respectively, in the cases with and without fast charging procedures. In summer time, most V2G procedures happen in the morning (i.e., before 6 a.m.) and early afternoon (i.e., before 3 p.m.). In winter time, most V2G selling occurs in the morning and lasts for longer time than in the summer time. But in the case without fast charging, V2G happens both in the morning and early afternoon. As for the "random" structure, compared with Figure 4(a), we notice that most of V2G happens in the morning, when most idle EVs present without V2G options. That is, V2G helps to utilize vehicle idle time, which can also be reflected in the idle cost reduction in Table 4.

6. Conclusions

In this paper, we studied EV sharing systems integrated with V2G. We formulated the problem of optimal service zone planning and EV fleet deployment under uncertain rental demand and electricity price as a two-stage stochastic integer program. We developed Benders decomposition and scenario decomposition algorithms to efficiently solve this computationally challenging problem. Via numerical study using real-world and synthetic data, we drew insights into the values of V2G integration in different aspects. We found that integrating V2G in EV sharing systems can significantly benefit the service provider through increased profitability. Furthermore, the benefit of V2G can withstand the impact of battery degradation and can be more significant when there is more severe traffic congestion, or when the urban spatial structure has concentrated business/residential areas. V2G integration (complemented by fast charging technology) can also benefit carshare users through improvement in the quality of service. With respect to socioenvironmental benefit, V2G integration results in more EV deployment and larger battery capacities, which in turn facilitates the adoption of EV sharing and reduces private car ownership and GHG emissions. A shared EV fleet equipped with V2G selling can also provide substantial flexible capacity to the power grid.

Our model can be extended in several ways. First, we can formulate a multistage dynamic program and obtain real-time operational solutions via linear-decision-rule-based approximation (see Online Appendix E). Second, our current model is formulated for designing a new EV sharing system from scratch. It can be easily modified to handle system reoptimization and/or expansion with existing facilities and deployed vehicle fleets. Third, the service-level requirement is enforced by penalty cost in our model. It is possible to adopt a chance constraint formulation to provide more explicit service-level guarantees. For future research, it is possible to apply other methodologies, such as approximate dynamic programming, to provide real-time decision support to large-scale systems. It is also interesting to study adaptive robust analogues of this problem to address the high level of ambiguity in carsharing demand and electricity price.

Acknowledgments

The authors are grateful for constructive feedback and suggestions given by reviewers and the Associate Editor. The authors are grateful for support from the National Science Foundation.

Endnotes

[1] See https://uk.nissannews.com/en-GB/releases/release-145248-nissan-and-enel-launch-groundbreaking-vehicle-to-grid-project-in-the-uk.

[2] See https://www.car2go.com/NL/en/amsterdam/ and https://www.car2go.com/ES/en/madrid/.

[3] See https://www.mpoweruk.com/infrastructure.htm.

[4] See www.open-mpi.org/.

References

Agrawal VV, Bellos I (2016) The potential of servicizing as a green business model. *Management Sci.* 63(5):1545–1562.

Aguirre K, Eisenhardt L, Lim C, Nelson B, Norring A, Slowik P, Tu N (2012) Lifecycle analysis comparison of a battery electric vehicle and a conventional gasoline vehicle. Report, California Air Resources Board, Sacramento, CA.

Ahmad M, Musirin I, Othman M (2013) Profit determination for vehicle-to-grid (V2G) operation in smart grid environment. *2013 IEEE 7th Internat. Power Engrg. Optim. Conf. (PEOCO)* (IEEE, Piscataway, NJ), 758–763.

Ahmed S (2013) A scenario decomposition algorithm for 0-1 stochastic programs. *Oper. Res. Lett.* 41(6):565–569.

Barrios J, Godier J (2014) Fleet sizing for flexible carsharing systems: Simulation-based approach. *Transportation Res. Record J. Transportation Res. Board* 2416(1):1–9.

Barth M, Todd M (1999) Simulation model performance analysis of a multiple station shared vehicle system. *Transportation Res. Part C: Emerging Tech.* 7(4):237–259.

Bellos I, Ferguson M, Toktay LB (2017) The car sharing economy: Interaction of business model choice and product line design. *Manufacturing Service Oper. Management* 19(2):185–201.

Benders JF (1962) Partitioning procedures for solving mixed-variables programming problems. *Numerische Mathematik* 4(1):238–252.

Benjaafar S, Bernhard H, Courcoubetis C (2017a) Drivers, riders and service providers: The impact of the sharing economy on mobility. *Proc. 12th Workshop Econom. Networks Systems Comput.* (ACM, New York), Article No. 1.

Benjaafar S, Kong G, Li X, Courcoubetis C (2019) Peer-to-peer product sharing: Implications for ownership, usage, and social welfare in the sharing economy. *Management Sci.* 65(2):477–493.

Benjaafar S, Li X, Li X (2017b) Dynamic inventory repositioning in on-demand rental networks. Preprint, submitted March 30, http://dx.doi.org/10.2139/ssrn.2942921.

Biondi E, Boldrini C, Bruno R (2016) Optimal charging of electric vehicle fleets for a car sharing system with power sharing. *2016 IEEE Internat. Energy Conf. (ENERGYCON)* (IEEE, Piscataway, NJ), 1–6.

Birge JR, Louveaux FV (2011) *Introduction to Stochastic Programming* (Springer, New York).

Bondorová B, Archer G (2017) Does sharing cars really reduce car use? Report, Transport and Environment, Brussels, Belgium.

Boyacı B, Zografos KG, Geroliminis N (2015) An optimization framework for the development of efficient one-way car-sharing systems. *Eur. J. Oper. Res.* 240(3):718–733.

Chang J, Yu M, Shen S, Xu M (2017) Location design and relocation of mixed shared cars. *Service Sci.* 9(3):205–218.

Cheung RK, Chen CY (1998) A two-stage stochastic network model and solution methods for the dynamic empty container allocation problem. *Transportation Sci.* 32(2):142–162.

Douris C (2017) Electric vehicle-to-grid services can feed, stabilize power supply. *Forbes* (December 18), https://www.forbes.com/sites/constancedouris/2017/12/18/electric-vehicle-to-grid-services-can-feed-stabilize-power-supply/.

Fournier G, Lindenlauf F, Baumann M, Seign R, Weil M (2014) Carsharing with electric vehicles and vehicle-to-grid: A future business model? Proff H, ed. *Radikale Innovationen in der Mobilität* (Springer, Wiesbaden, Germany), 63–79.

Fournier G, Seign R, Goehlich V, Bogenberger K (2015) Car-sharing with electric vehicles: A contribution to sustainable mobility. *Interdisziplinäre Managementforschung* 11:955–975.

Glotz-Richter M (2016) Reclaim street space!–exploit the European potential of car sharing. *Transportation Res. Procedia* 14: 1296–1304.

He L, Hu Z, Zhang M (2020) Robust repositioning for vehicle sharing. *Manufacturing Service Oper. Management* 22(2):241–256.

He L, Ma G, Qi W, Wang X (2018) Charging electric vehicle sharing fleet. Preprint, submitted August 15, http://dx.doi.org/10.2139/ssrn.3223735.

He L, Mak HY, Rong Y, Shen ZJM (2017) Service region design for urban electric vehicle sharing systems. *Manufacturing Service Oper. Management* 19(2):309–327.

Kempton W, Tomić J (2005) Vehicle-to-grid power implementation: From stabilizing the grid to supporting large-scale renewable energy. *J. Power Sources* 144(1):280–294.

Kleywegt AJ, Shapiro A, Homem-de Mello T (2002) The sample average approximation method for stochastic discrete optimization. *SIAM J. Optim.* 12(2):479–502.

Lambert F (2018) Tesla could 'revisit' vehicle-to-grid technology, says Elon Musk. *Electrek* (July 5), https://electrek.co/2018/07/05/tesla-vehicle-to-grid-technology-v2g-elon-musk/.

Lauinger D, Vuille F, Kuhn D (2017) A review of the state of research on vehicle-to-grid (V2G): Progress and barriers to deployment. Working paper, École Polytechnique Fédérale de Lausanne Lausanne, Switzerland.

Lim MK, Mak HY, Rong Y (2014) Toward mass adoption of electric vehicles: Impact of the range and resale anxieties. *Manufacturing Service Oper. Management* 17(1):101–119.

Lu M, Chen Z, Shen S (2018) Optimizing the profitability and quality of service in carshare systems under demand uncertainty. *Manufacturing Service Oper. Management* 20(2):162–180.

Lund H, Kempton W (2008) Integration of renewable energy into the transport and electricity sectors through V2G. *Energy Policy* 36(9):3578–3587.

Mak HY, Rong Y, Shen ZJM (2013) Infrastructure planning for electric vehicles with battery swapping. *Management Sci.* 59(7): 1557–1575.

Nair R, Miller-Hooks E (2011) Fleet management for vehicle sharing operations. *Transportation Sci.* 45(4):524–540.

Peterson SB, Whitacre J, Apt J (2010) The economics of using plug-in hybrid electric vehicle battery packs for grid storage. *J. Power Sources* 195(8):2377–2384.

Salmerón J, Apte A (2010) Stochastic optimization for natural disaster asset prepositioning. *Production Oper. Management* 19(5): 561–574.

Shaheen S, Sperling D, Wagner C (1998) Carsharing in Europe and North America: Past, present, and future. *Transportation Quart.* 52(3):35–52.

Shapiro A, Homem-de-Mello T (2000) On the rate of convergence of optimal solutions of Monte Carlo approximations of stochastic programs. *SIAM J. Optim.* 11(1):70–86.

Sovacool BK, Hirsh RF (2009) Beyond batteries: An examination of the benefits and barriers to plug-in hybrid electric vehicles (PHEVs) and a vehicle-to-grid (V2G) transition. *Energy Policy* 37(3): 1095–1103.

Steitz C (2018) Nissan LEAF gets approval for vehicle-to-grid use in Germany. *Reuters* (October 23), https://www.reuters.com/article/us-autos-electricity-germany/nissan-leaf-approved-for-vehicle-to-grid-use-in-germany-idUSKCN1MX1AH.

Tan KM, Ramachandaramurthy VK, Yong JY (2016) Integration of electric vehicles in smart grid: A review on vehicle to grid technologies and optimization techniques. *Renewable Sustainable Energy Rev.* 53:720–732.

Turton H, Moura F (2008) Vehicle-to-grid systems for sustainable development: An integrated energy analysis. *Tech. Forecasting Social Change* 75(8):1091–1108.

Zhou C, Qian K, Allan M, Zhou W (2011) Modeling of the cost of EV battery wear due to V2G application in power systems. *IEEE Trans. Engineering Conversion* 26(4):1041–1050.